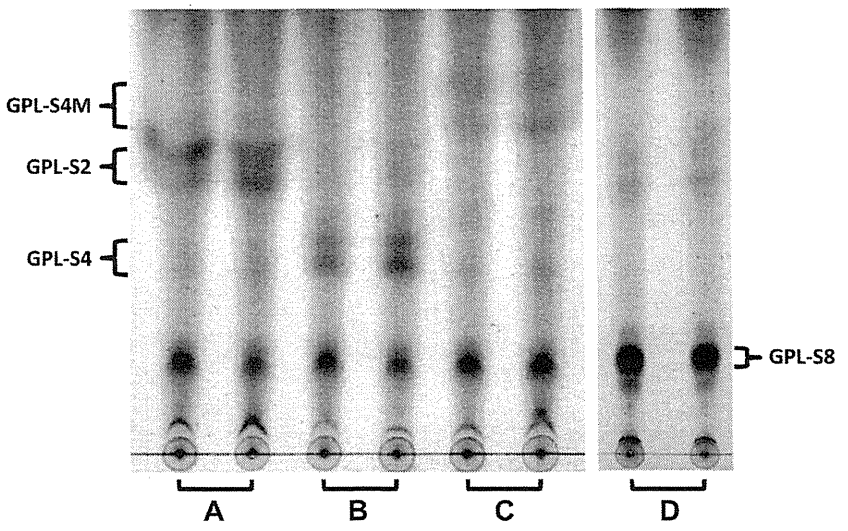

FIG. 2. TLC analysis of crude GPL extracts from recombinant *M. smegmatis* strains MS-S2/pYM301a (A), MS-S2/pYM-hlpA (B), MS-S2/pYM-hlpA-orf2 (C), and MS-S2/pYM-orf3-orf4-orf5 (D). GPL extracts were prepared from the total lipid fraction after a mild alkaline hydrolysis step. Each recombinant strain was tested by two samples derived from independent colonies. Samples were spotted and developed in $CHCl_3$-CH_3OH-H_2O (30:8:1 [vol/vol/vol]).

presence or absence of the methyl group in the fatty acid portion as described above. Thus, the results revealed that the mass unit difference between GPL-S2 (*m/z* 1,465.80, 1,479.82) and GPL-S4 (*m/z* 1,611.84, 1,625.85) was 146 and that between GPL-S2 and GPL-S4M (*m/z* 1,625.89, 1,639.90) was 160, demonstrating that the Rha and 4-*O*-Me-Rha residues were further added to the GPL-S2 to yield GPL-S4 and GPL-S4M, respectively.

The results from TLC, GC-MS, and MALDI-TOF MS analyses strongly suggested that *hlpA* and ORF2 are involved in the formation of 4-*O*-Me Rha. However, it is not clear whether the *hlpA* gene product functions as a glycosyltransferase that transfers a Rha via 1→4 linkage to a Fuc residue, which is observed only for serovar 4-specific GPL. To elucidate the function of *hlpA*, we determined the linkage of sugar moieties of GPL-S4 produced by recombinant strain MS-S2/pYM-hlpA (Fig. 2, lane B). The purified GPL-S4 was subjected to perdeuteriomethylation followed by GC-MS and gave four peaks corresponding to Fuc, 6-d-Tal, Rha, and 2,3,4-tri-*O*-Me-Rha (data not shown). The spectra of Rha and 6-d-Tal demonstrated that the linkage position between these two sugar residues is commonly observed in the oligosaccharide of all ssGPLs, and position C-3 of Rha is linked to the next one, which is consistent with the data previously reported (Fig. 5B and C) (25, 26). In addition, the detection of fragment ions at *m/z* 121, 168, and 206 in spectra of Fuc indicated that its positions C-2 and C-3 were deuteriomethylated (Fig. 5D), meaning that position C-1 of Fuc is linked to position C-3 of Rha and position C-4 of Fuc is linked to the next one. These observations were supported by the fact that GPL-S4 was structurally based on the oligosaccharide of serovar 2-specific GPL. The peak of 2,3,4-tri-*O*-Me-Rha was found to include mixed fragment ions (Fig. 5A). A group of fragment ions corresponding to the spectra of 2,3,4-tri-*O*-Me-Rha linked to alaninol of tetrapeptide was observed. The remaining fragment ions at *m/z* 121, 134, 168, and 181 indicate the presence of deuteriomethyl groups at positions C-2, C-3, and C-4 of the other Rha that is linked at the terminus of oligosaccharide in GPL-S4. These results indicate that position C-1 of terminal Rha is linked to position C-4 of Fuc. Accordingly, the oligosaccharide structures of GPL-S4 were determined to have Rha-(1→4)-Fuc-(1→3)-Rha-(1→2)-6-d-Tal at D-*allo*-Thr, demonstrating that *hlpA* encodes a rhamnosyltransferase that transfers a Rha residue via 1→4 linkage to a Fuc residue of serovar 2-specific GPL (Fig. 6).

DISCUSSION

It is known that serovar 4 is the most prevalent type, and serovar 4-specific GPL, particularly its oligosaccharide portion, plays a role in exhibiting the specific properties that belong to pathogenic factors. However, to date, the biosynthesis of its oligosaccharide portion has not been clarified. In this study, structural determination of three recombinant products, GPL-S2, GPL-S4, and GPL-S4M, revealed that *hlpA* and its downstream gene (ORF2) in the GPL biosynthetic gene cluster are involved in the formation of 4-*O*-methyl Rha, which is unique to serovar 4-specific GPL (Fig. 6). Previously, it was reported that the GPL biosynthetic gene cluster of MAC serovar 2 strains contained one gene whose amino acid sequences are similar to that of *hlpA* with 69% identity (14). This has been regarded as the gene not associated with GPL biosynthesis, because its amino acid sequences are similar to those of hemolytic proteins distributed in some species of bacteria (4). Thus, as shown in Fig. 6, it was surprising that *hlpA* from serovar 4 was found to encode a rhamnosyltransferase that plays a critical role in the pathway leading from serovar 2-specific GPL to serovar 4-specific GPL. For mycobacterium species, a BLAST analysis of HlpA revealed that its homologues are seen only in MAC serovar 2 and not in other species, including *Mycobacterium tuberculosis*. When we tested the

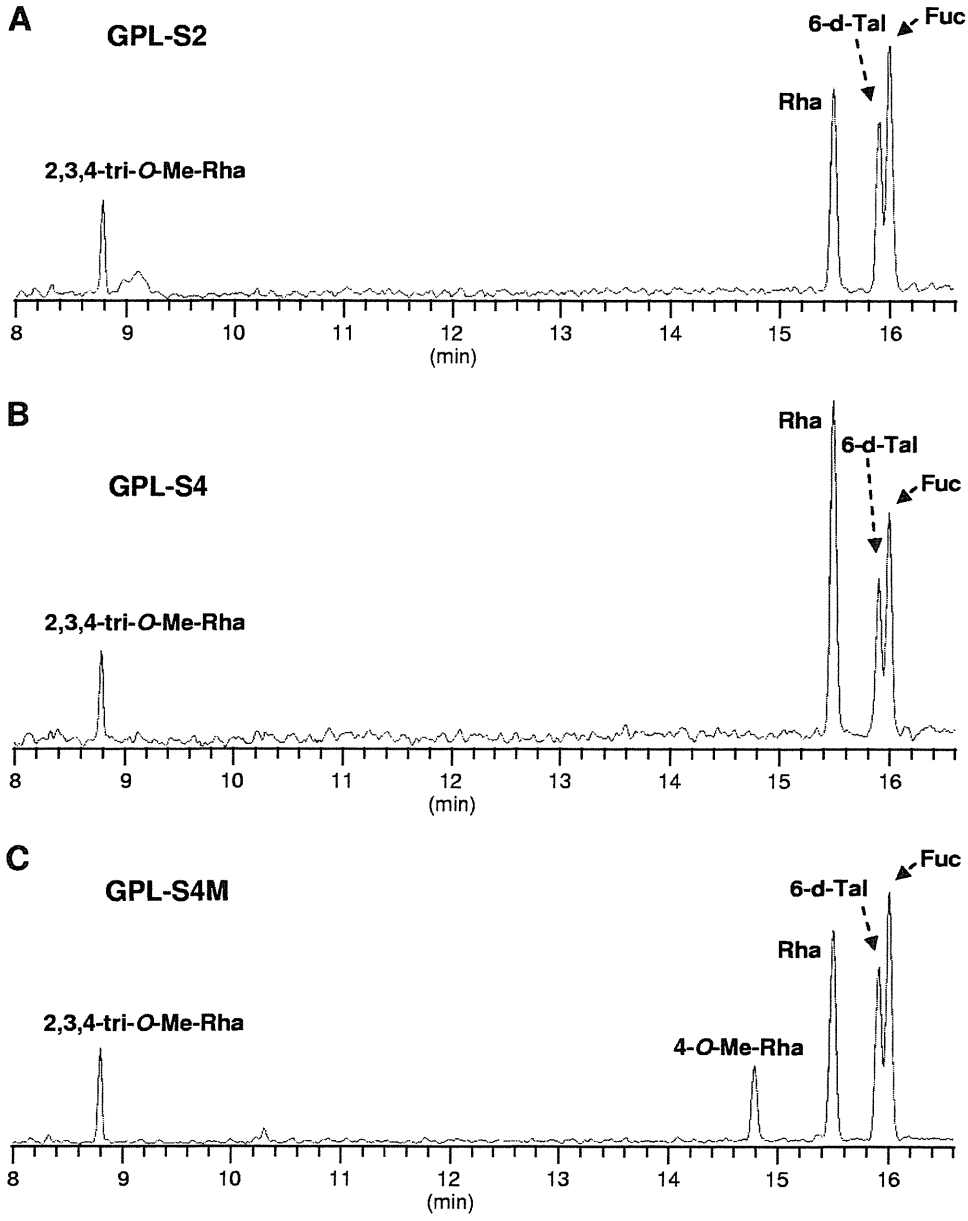

FIG. 3. GC-MS of alditol acetate derivatives from GPL-S2 (A), GPL-S4 (B), and GPL-S4M (C), which were purified from GPL extracts of recombinant *M. smegmatis* strains MS-S2/pYM301a, MS-S2/pYM-hlpA, and MS-S2/pYM-hlpA-orf2, respectively.

function of HlpA from serovar 2, it did not serve as a glycosyltransferase like HlpA from serovar 4 (data not shown). At present, the function of HlpA from serovar 2 is still unclear, because the biosynthesis of the oligosaccharide portion in serovar 2-specific GPL has been fully elucidated (14, 26). The oligosaccharide structure of serovar 2-specific GPL is basic for several ssGPLs, including serovar 4-specific GPL. In the biosynthetic gene cluster of serovar 2-specific GPL, several insertion sequence (IS) elements are observed, raising the possibility that the HlpA from serovar 2 is retained through genomic alterations that induce biosynthetic changes from other ssGPLs to serovar 2-specific GPL. Therefore, HlpA in the serovar 2 strain originally might function as a glycosyltransferase in the biosynthesis of oligosaccharides of other serovars.

Most HlpA homologues are putatively categorized as hemolytic proteins because they are similar to one protein from *Prevotella intermedia*, which is actually proved to have hemolytic activity (4). Since the amino acid sequences of HlpA show 38% identity and 54% similarity to the above protein of *P. intermedia*, we predicted that HlpA also possesses hemolytic activity as an additional function. However, none was detected when *hlpA* was expressed in *M. smegmatis* and *E. coli* by plate assay using a sheep blood agar plate (data not shown). A BLAST analysis of HlpA homologues showed that they also

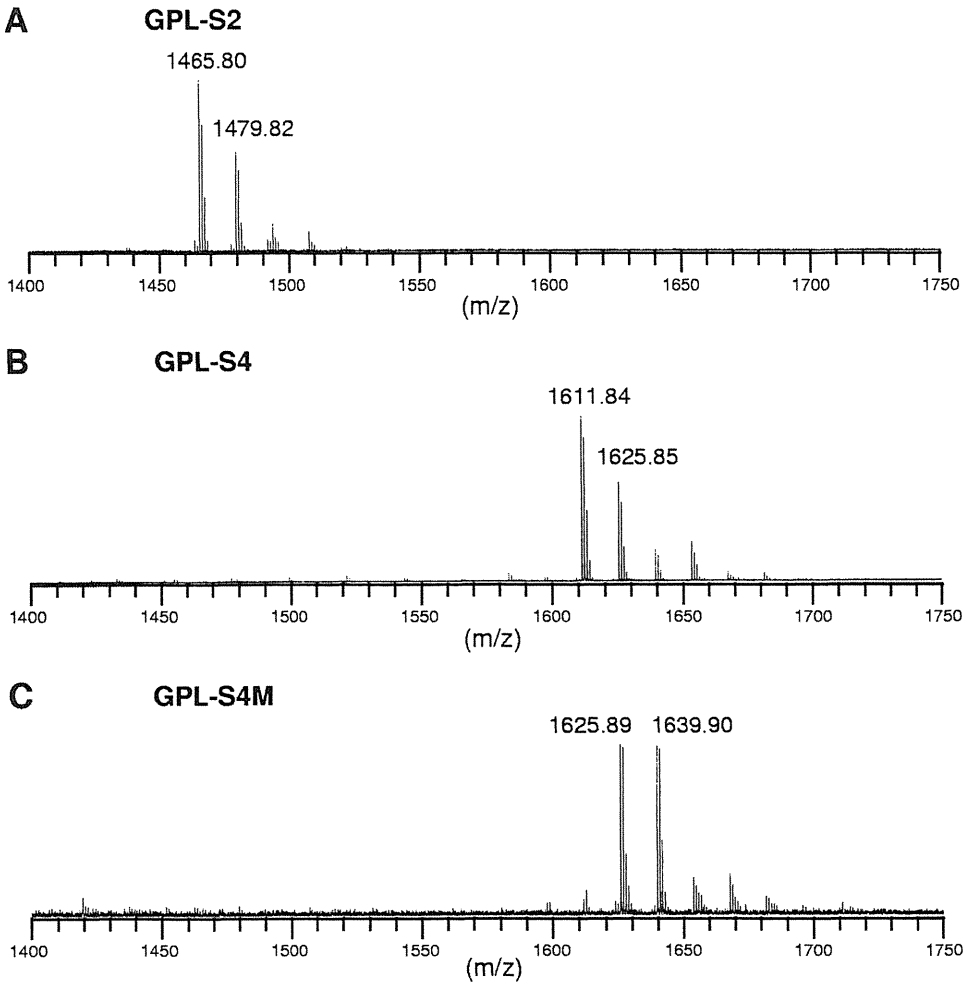

FIG. 4. MALDI-TOF MS of GPL-S2 (A), GPL-S4 (B), and GPL-S4M (C), which were purified from GPL extracts of recombinant *M. smegmatis* strains MS-S2/pYM301a, MS-S2/pYM-hlpA, and MS-S2/pYM-hlpA-orf2, respectively.

contained a partial motif of some glycosyltransferases and methyltransferases. Therefore, it is envisaged that the evolutionary ancestor of HlpA might have lost hemolytic activity in MAC or, conversely, have been altered to retain it in *P. intermedia* in the course of phylogenetic evolution between these bacterial species.

Serovar 4 strains, including ATCC 35767, have been recognized as strains producing the serovar 4-specific GPL but not the serovar 8-specific GPL (24, 35). However, as shown in Fig. 1, we found that the GPL biosynthetic gene cluster contains three known genes (the ORF3, ORF4, and ORF5 genes) previously identified as biosynthetic genes responsible for the formation of 4,6-*O*-(1-carboxyethylidene)-3-*O*-methyl glucose residue in the oligosaccharide of serovar 8-specific GPL (25). TLC analysis showed that overexpression of three ORFs potentially produces the serovar 8-specific GPL, including the 4,6-*O*-(1-carboxyethylidene)-3-*O*-methyl glucose residue (Fig. 2, lane D), demonstrating that in the serovar 4 strain, there is inefficient expression of three genes, which might be caused by genomic alterations affecting their transcription, resulting in the loss of serovar 8-specific GPL. Moreover, HlpA homologues are often found in several species of cyanobacteria but not in other bacterial groups and mycobacterium species, implying the occurrence of a certain kind of "horizontal gene transfer" between these environmental bacteria. Thus, MAC seemed to incorporate foreign genes or realign preexisting genes to modify the oligosaccharide structures of GPLs for their survival in a varied environment. In terms of sugar composition and linkage affecting the properties of ssGPLs, the functional aspects of the 4-*O*-methyl-Rha residue, which influence the interactions with the host cell, are still unclear. In addition, the sugar linkage Rha-(1→4)-Fuc is seen only in serovar 4-specific GPL and not in other ssGPLs, suggesting that it might generate unique properties that differ notably from those generated by other sugar linkages. Also, the rarity of this sugar linkage could be one of the factors that define the specificity of MAC serovar 4, which would be resolved by further studies, including the generation of an *hlpA* knockout mutant. For functional characterization of *hlpA* and ORF2, we have adopted the gene expression experiment

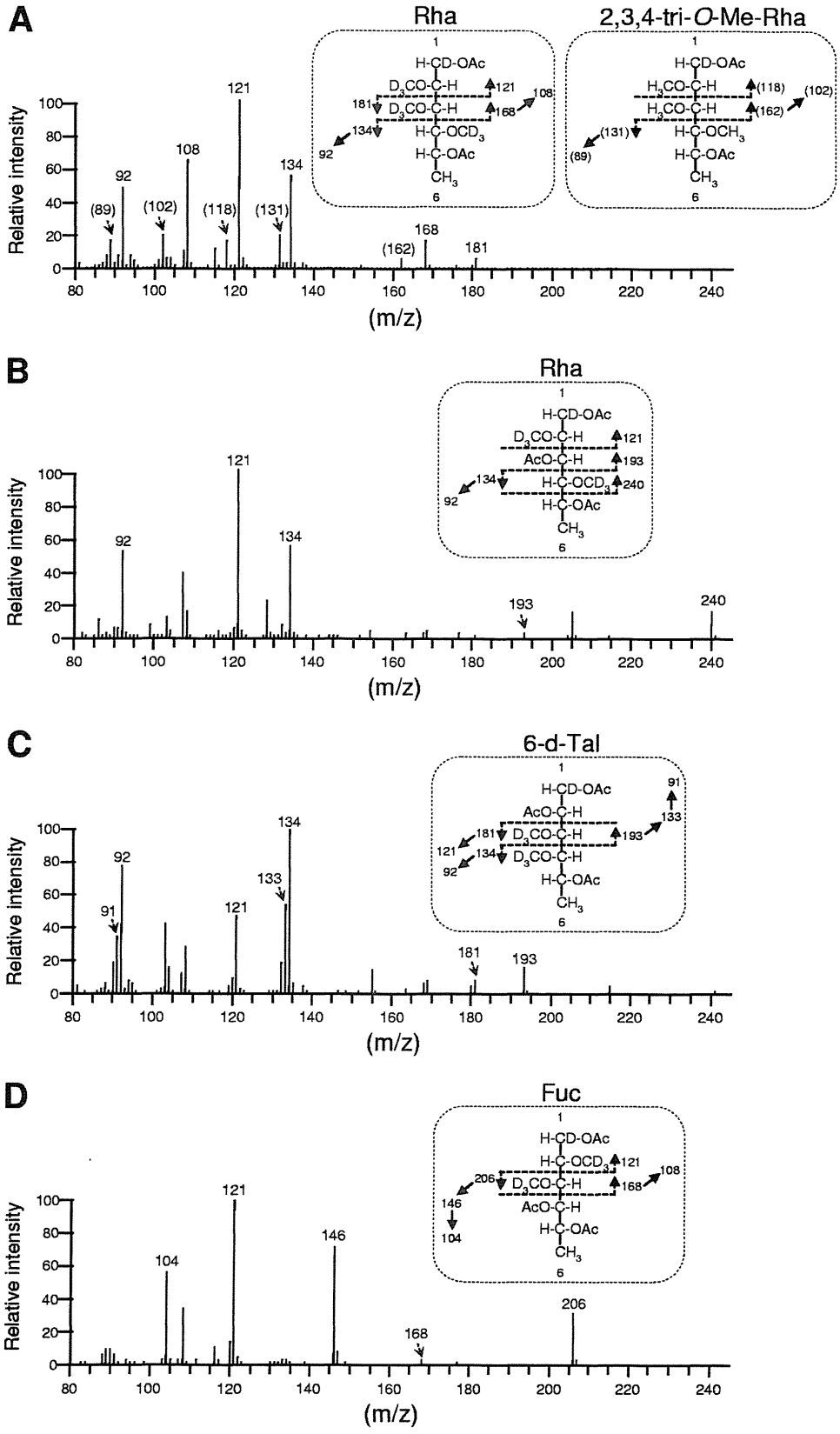

FIG. 5. GC-MS spectra and fragment ion assignments of 2,3,4-tri-*O*-Me-Rha (A), Rha (A and B), 6-*d*-Tal (C), and Fuc (D), which are derived from alditol acetates of sugars released from deuteriomethylated GPL-S4. Ac, acetate; D, deuterium.

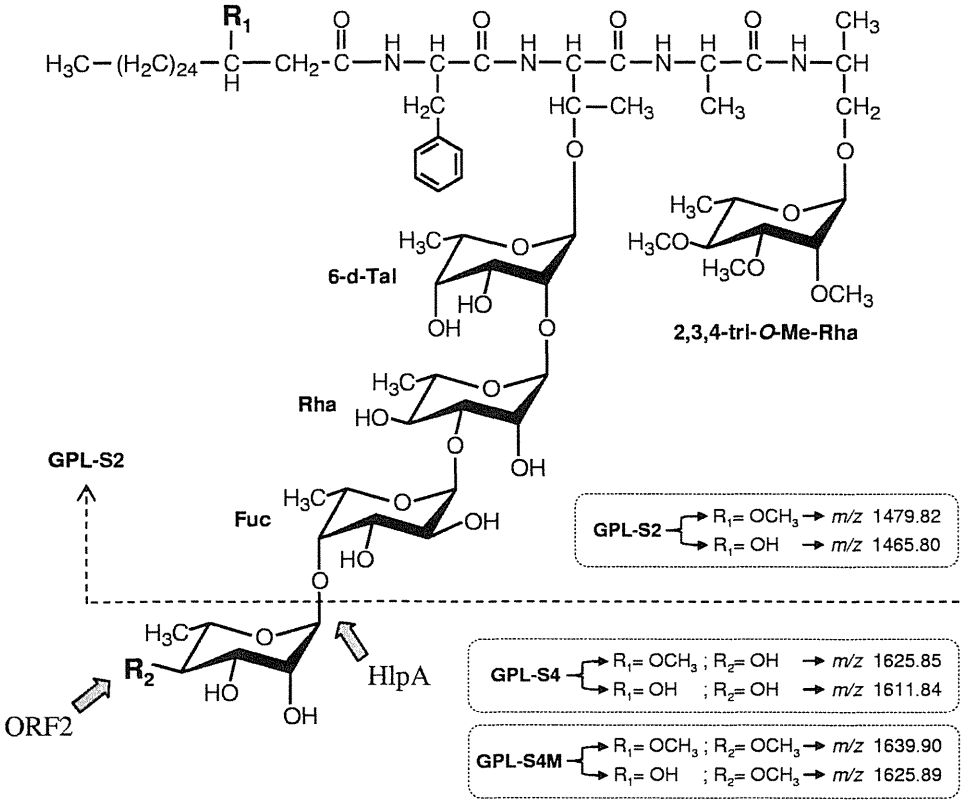

FIG. 6. Proposed structures and biosynthetic pathways for GPL-S2, GPL-S4, and GPL-S4M. Parentheses indicate structural differences between three compounds, which are deduced from MALDI-TOF MS analyses {pseudomolecular ions ($[M + Na]^+$)}.

using the *M. smegmatis* strain. Further enzymatic analyses, such as *in vitro* testing with recombinant proteins, would confirm our results. Taken together, these findings may contribute to understanding the mechanism for generation of structural and functional diversity of GPLs as well as their biological role in MAC.

ACKNOWLEDGMENTS

This research was partially supported by a Grant-in-Aid for Young Scientists (B) from the Ministry of Education, Culture, Science and Technology of Japan and by a Research on Emerging and Re-Emerging Infectious Diseases grant from the Ministry of Health, Labor and Welfare of Japan.

REFERENCES

1. **Askgaard, D. S., S. B. Giese, S. Thybo, A. Lerche, and J. Bennedsen.** 1994. Serovars of *Mycobacterium avium* complex isolated from patients in Denmark. J. Clin. Microbiol. **32:**2880–2882.
2. **Aspinall, G. O., D. Chatterjee, and P. J. Brennan.** 1995. The variable surface glycolipids of mycobacteria: structures, synthesis of epitopes, and biological properties. Adv. Carbohydr. Chem. Biochem. **51:**169–242.
3. **Barrow, W. W., T. L. Davis, E. L. Wright, V. Labrousse, M. Bachelet, and N. Rastogi.** 1995. Immunomodulatory spectrum of lipids associated with *Mycobacterium avium* serovar 8. Infect. Immun. **63:**126–133.
4. **Beem, J. E., W. E. Nesbitt, and K. P. Leung.** 1999. Cloning of *Prevotella intermedia* loci demonstrating multiple hemolytic domains. Oral Microbiol. Immunol. **14:**143–152.
5. **Belisle, J. T., K. Klaczkiewicz, P. J. Brennan, W. R. Jacobs, Jr., and J. M. Inamine.** 1993. Rough morphological variants of *Mycobacterium avium*: characterization of genomic deletions resulting in the loss of glycopeptidolipid expression. J. Biol. Chem. **268:**10517–10523.
6. **Birkness, K. A., W. E. Swords, P. H. Huang, E. H. White, C. S. Dezzutti, R. B. Lal, and F. D. Quinn.** 1999. Observed differences in virulence-associated phenotypes between a human clinical isolate and a veterinary isolate of *Mycobacterium avium*. Infect. Immun. **67:**4895–4901.
7. **Bjorndal, H., C. G. Hellerqvist, B. Lindberg, and S. Svensson.** 1970. Gas-liquid chromatography and mass spectrometry in methylation analysis of polysaccharides. Angew. Chem. Internat. Ed. Engl. **9:**610–619.
8. **Brennan, P. J., and H. Nikaido.** 1995. The envelope of mycobacteria. Annu. Rev. Biochem. **64:**29–63.
9. **Camphausen, R. T., R. L. Jones, and P. J. Brennan.** 1986. Structure and relevance of the oligosaccharide hapten of *Mycobacterium avium* serotype 2. J. Bacteriol. **168:**660–667.
10. **Chatterjee, D., and K. H. Khoo.** 2001. The surface glycopeptidolipids of mycobacteria: structures and biological properties. Cell. Mol. Life Sci. **58:** 2018–2042.
11. **Ciucanu, I., and F. Kerek.** 1984. A simple and rapid method for the permethylation of carbohydrates. Carbohydr. Res. **131:**209–217.
12. **Daffe, M., and P. Draper.** 1998. The envelope layers of mycobacteria with reference to their pathogenicity. Adv. Microb. Physiol. **39:**131–203.
13. **Daffe, M., M. A. Laneelle, and G. Puzo.** 1983. Structural elucidation by field desorption and electron-impact mass spectrometry of the C-mycosides isolated from *Mycobacterium smegmatis*. Biochim. Biophys. Acta **751:**439–443.
14. **Eckstein, T. M., J. T. Belisle, and J. M. Inamine.** 2003. Proposed pathway for the biosynthesis of serovar-specific glycopeptidolipids in *Mycobacterium avium* serovar 2. Microbiology **149:**2797–2807.
15. **Eckstein, T. M., F. S. Silbaq, D. Chatterjee, N. J. Kelly, P. J. Brennan, and J. T. Belisle.** 1998. Identification and recombinant expression of a *Mycobacterium avium* rhamnosyltransferase gene (*rtfA*) involved in glycopeptidolipid biosynthesis. J. Bacteriol. **180:**5567–5573.
16. **Fujiwara, N., N. Nakata, S. Maeda, T. Naka, M. Doe, I. Yano, and K. Kobayashi.** 2007. Structural characterization of a specific glycopeptidolipid containing a novel *N-acyl*-deoxy sugar from *Mycobacterium intracellulare* serotype 7 and genetic analysis of its glycosylation pathway. J. Bacteriol. **189:**1099–1108.
17. **Fujiwara, N., N. Nakata, T. Naka, I. Yano, M. Doe, D. Chatterjee, M. McNeil, P. J. Brennan, K. Kobayashi, M. Makino, S. Matsumoto, H. Ogura, and S. Maeda.** 2008. Structural analysis and biosynthesis gene cluster of an antigenic glycopeptidolipid from *Mycobacterium intracellulare*. J. Bacteriol. **190:**3613–3621.
18. **Horgen, L., E. L. Barrow, W. W. Barrow, and N. Rastogi.** 2000. Exposure of human peripheral blood mononuclear cells to total lipids and serovar-spe-

cific glycopeptidolipids from *Mycobacterium avium* serovars 4 and 8 results in inhibition of TH1-type responses. Microb. Pathog. **29:**9–16.
19. **Jeevarajah, D., J. H. Patterson, M. J. McConville, and H. Billman-Jacobe.** 2002. Modification of glycopeptidolipids by an *O*-methyltransferase of *Mycobacterium smegmatis*. Microbiology **148:**3079–3087.
20. **Julander, I., S. Hoffner, B. Petrini, and L. Ostlund.** 1996. Multiple serovars of *Mycobacterium avium* complex in patients with AIDS. APMIS **104:**318–320.
21. **Kano, H., T. Doi, Y. Fujita, H. Takimoto, I. Yano, and Y. Kumazawa.** 2005. Serotype-specific modulation of human monocyte functions by glycopeptidolipid (GPL) isolated from *Mycobacterium avium* complex. Biol. Pharm. Bull. **28:**335–339.
22. **Krzywinska, E., and J. S. Schorey.** 2003. Characterization of genetic differences between *Mycobacterium avium* subsp. *avium* strains of diverse virulence with a focus on the glycopeptidolipid biosynthesis cluster. Vet. Microbiol. **91:**249–264.
23. **Maekura, R., Y. Okuda, A. Hirotani, S. Kitada, T. Hiraga, K. Yoshimura, I. Yano, K. Kobayashi, and M. Ito.** 2005. Clinical and prognostic importance of serotyping *Mycobacterium avium-Mycobacterium intracellulare* complex isolates in human immunodeficiency virus-negative patients. J. Clin. Microbiol. **43:**3150–3158.
24. **McNeil, M., A. Y. Tsang, and P. J. Brennan.** 1987. Structure and antigenicity of the specific oligosaccharide hapten from the glycopeptidolipid antigen of *Mycobacterium avium* serotype 4, the dominant mycobacterium isolated from patients with acquired immune deficiency syndrome. J. Biol. Chem. **262:**2630–2635.
25. **Miyamoto, Y., T. Mukai, Y. Maeda, M. Kai, T. Naka, I. Yano, and M. Makino.** 2008. The *Mycobacterium avium* complex *gtfTB* gene encodes a glucosyltransferase required for the biosynthesis of serovar 8-specific glycopeptidolipid. J. Bacteriol. **190:**7918–7924.
26. **Miyamoto, Y., T. Mukai, Y. Maeda, N. Nakata, M. Kai, T. Naka, I. Yano, and M. Makino.** 2007. Characterization of the fucosylation pathway in the biosynthesis of glycopeptidolipids from *Mycobacterium avium* complex. J. Bacteriol. **189:**5515–5522.
27. **Miyamoto, Y., T. Mukai, F. Takeshita, N. Nakata, Y. Maeda, M. Kai, and M. Makino.** 2004. Aggregation of mycobacteria caused by disruption of fibronectin-attachment protein-encoding gene. FEMS Microbiol. Lett. **236:**227–234.
28. **Patterson, J. H., M. J. McConville, R. E. Haites, R. L. Coppel, and H. Billman-Jacobe.** 2000. Identification of a methyltransferase from *Mycobacterium smegmatis* involved in glycopeptidolipid synthesis. J. Biol. Chem. **275:**24900–24906.
29. **Snapper, S. B., R. E. Melton, S. Mustafa, T. Kieser, and W. R. Jacobs, Jr.** 1990. Isolation and characterization of efficient plasmid transformation mutants of *Mycobacterium smegmatis*. Mol. Microbiol. **4:**1911–1919.
30. **Sweet, L., and J. S. Schorey.** 2006. Glycopeptidolipids from *Mycobacterium avium* promote macrophage activation in a TLR2- and MyD88-dependent manner. J. Leukoc. Biol. **80:**415–423.
31. **Sweet, L., W. Zhang, H. Torres-Fewell, A. Serianni, W. Boggess, and J. Schorey.** 2008. *Mycobacterium avium* glycopeptidolipids require specific acetylation and methylation patterns for signaling through toll-like receptor 2. J. Biol. Chem. **283:**33221–33231.
32. **Tassell, S. K., M. Pourshafie, E. L. Wright, M. G. Richmond, and W. W. Barrow.** 1992. Modified lymphocyte response to mitogens induced by the lipopeptide fragment derived from *Mycobacterium avium* serovar-specific glycopeptidolipids. Infect. Immun. **60:**706–711.
33. **Tsang, A. Y., J. C. Denner, P. J. Brennan, and J. K. McClatchy.** 1992. Clinical and epidemiological importance of typing of *Mycobacterium avium* complex isolates. J. Clin. Microbiol. **30:**479–484.
34. **Vergne, I., and M. Daffe.** 1998. Interaction of mycobacterial glycolipids with host cells. Front. Biosci. **3:**d865–876.
35. **Wayne, L. G., R. C. Good, A. Tsang, R. Butler, D. Dawson, D. Groothuis, W. Gross, J. Hawkins, J. Kilburn, M. Kubin, K. H. Schroder, V. A. Silcox, C. Smith, M. F. Thorel, C. Woodley, and M. A. Yakrus.** 1993. Serovar determination and molecular taxonomic correlation in *Mycobacterium avium*, *Mycobacterium intracellulare*, and *Mycobacterium scrofulaceum*: a cooperative study of the International Working Group on Mycobacterial Taxonomy. Int. J. Syst. Bacteriol. **43:**482–489.
36. **Yakrus, M. A., and R. C. Good.** 1990. Geographic distribution, frequency, and specimen source of *Mycobacterium avium* complex serotypes isolated from patients with acquired immunodeficiency syndrome. J. Clin. Microbiol. **28:**926–929.

Microbial Pathogenesis 49 (2010) 181–185

Contents lists available at ScienceDirect

Microbial Pathogenesis

journal homepage: www.elsevier.com/locate/micpath

Analysis of *Mycobacterium leprae* gene expression using DNA microarray

Takeshi Akama, Kazunari Tanigawa, Akira Kawashima, Huhehasi Wu, Norihisa Ishii, Koichi Suzuki*

Leprosy Research Center, National Institute of Infectious Diseases, 4-2-1 Aoba-cho, Higashimurayama-shi, Tokyo 189-0002, Japan

ARTICLE INFO

Article history:
Received 8 February 2010
Received in revised form
19 May 2010
Accepted 20 May 2010
Available online 27 May 2010

Keywords:
Mycobacterium leprae
Leprosy
DNA microarray
Operon

ABSTRACT

Mycobacterium leprae, the causative agent of leprosy, does not grow under *in vitro* condition, making molecular analysis of this bacterium difficult. For this reason, bacteriological information regarding *M. leprae* gene function is limited compared with other mycobacterium species. In this study, we performed DNA microarray analysis to clarify the RNA expression profile of the Thai53 strain of *M. leprae* grown in footpads of hypertensive nude rats (SHR/NCrj-*rnu*). Of 1605 *M. leprae* genes, 315 showed signal intensity twofold higher than the median. These genes include Acyl-CoA metabolic enzymes and drug metabolic enzymes, which might be related to the virulence of *M. leprae*. In addition, consecutive RNA expression profile and *in silico* analyses enabled identification of possible operons within the *M. leprae* genome. The present results will shed light on *M. leprae* gene function and further our understanding of the pathogenesis of leprosy.

1. Introduction

Mycobacterium leprae (*M. leprae*) is the causative agent of leprosy, a chronic bacterial disease of the skin and nerves that still occurs at a relatively high incidence in South and Southeast Asia, South America, and Africa [1]. *M. leprae* grows in macrophages or Schwann cells upon *in vivo* infection; however, this bacterium has not been cultured *in vitro* to date [2]. Moreover, although nine-banded armadillos or nude mice have been used as limited models of *leprosy* [3], the mechanisms of infection, parasitization, proliferation, and pathogenesis of *M. leprae* have largely been undetermined. Previous studies on the nature of *M. leprae* were limited to methods requiring no gene manipulation, such as evaluation of respiration or ATP production [4], detection of RNA, or the use of other mycobacteria to study the function of specific *M. leprae* genes [5,6].

Whole genome sequence analysis of *M. leprae* has revealed that the genome consists of 3.3 Mbp and has only 1605 genes that encode proteins, but an unexpectedly large number of pseudogenes, that is, 1115 [7]. This genome sequence information has elucidated the evolutionary process of the *M. leprae* genome by phylogeographic analysis [8] or comparative genome science [9].

In order to clarify the expression profile of the entire *M. leprae* genome, as a first step, we previously performed membrane array analysis, then designed a whole genome tiling array analysis, and showed that high levels of RNA are transcribed from pseudogenes and other non-coding regions [10,11]. Tiling array was effective in detecting RNA expression from non-coding regions and pseudogenes, as well as in comparing the expression level between genes and non-coding regions. Nevertheless, the obtained signals in the array might have been affected by possible mismatch hybridization because of the low specificity of the tiling probes. This resulted in variable signal intensities of each probe even within the same gene. To date, precise analysis of *M. leprae* gene expression has been limited and a previous report utilized *Mycobacterium tuberculosis* (*M. tuberculosis*) open reading frame (ORF) array [12]. Moreover, little information is available regarding gene structures, such as operons.

In this study, we investigated the precise gene expression profile of *M. leprae* using an ORF array on which highly specific and multiple probes were mounted. We identified several functional genes whose expression level is significantly higher than that of other genes. We also found possible operon structures based on their consecutive expression and through the use of various prediction software packages.

2. Results

2.1. Evaluation of signal intensities of M. leprae ORF array

Total RNA was extracted from 7.2×10^{10} *M. leprae* cells grown in the footpad of SHR/NCrj-*rnu* rats and treated with DNase I. The ratio of 23S/16S rRNA was 0.83, indicating that the purified RNA was of sufficiently quality to proceed with array hybridization. Samples were then reverse-transcribed, fluorescence-labeled and

* Corresponding author. Tel.: +81 42 391 8211; fax: +81 42 394 9092.
E-mail address: koichis@nih.go.jp (K. Suzuki).

0882-4010/$ – see front matter © 2010 Elsevier Ltd. All rights reserved.
doi:10.1016/j.micpath.2010.05.010

hybridized with the ORF array. In this array, 20 different probes were designed for each of the 1605 *M. leprae* genes. These probes together with the multiple control probes were randomly arranged in one block on an array, and five different blocks were used for hybridization.

After scanning the array, the signal intensity of each probe ranged from 2^0 to 2^{16} (Fig. 1). From all the probes used, 19.7% showed signal intensity twofold higher than the median (*i.e.*, 5800 or $2^{12.5}$). Average signal intensity from 20 different probes in each gene was calculated for five different blocks. Genes with average signal intensity twofold higher than the median were considered as strongly positive. As a result, 315 genes were identified as highly expressed (Table S1). The expression of those genes was confirmed by RT-PCR and real-time PCR analysis for 28 and four genes, respectively (data not shown).

2.2. Expressed genes and their functional classes

M. leprae genes are classified into six functional classes [7]. To predict the characteristics of highly expressed genes, their functional classes were compared with those of the entire genes and pseudogenes (Fig. 2). The proportion of functional classes, whose RNA was detected strongly using ORF array, was found to be similar to that of the original gene classes, although there were some differences in the proportion of the six classes between genes and pseudogenes. This evidence suggests that all the six classes of *M. leprae* genes are similarly transcribed without significant preferences. Most of the genes detected by a previous tiling array analysis [10] were also detected using ORF array (92% matched).

Table 1 shows a more detailed expression profile of the functional gene classes. The average expression level of class III (Cell process) was the highest (27.3%), and that of class I (Small molecule metabolism) was the lowest (14.5%), although there was no significant difference. Interestingly, five out of the six genes expressed in class I.A were acyl-CoA metabolic enzymes, namely, ML0132, ML0138, ML0737, ML1241, and ML2358 (*fadD2*, *fadD28*, *fadE25*, *chA12*, and *fadD26*, respectively). Among the expressed genes, 12 showed more than tenfold stronger expression than the median (Table 2). Half of these genes belonged to Functional class II (Macromolecule metabolism); notably, four genes were from class II.C (Cell envelope). A putative monooxygenase showed the highest expression followed by hypothetical protein, which was 64–77% homologous to the *PadR* transcriptional regulator family of seven *Mycobacterium* species, namely, *Mycobacterium avium* (77%), *Mycobacterium marinum* (76%), *Mycobacterium ulcerans* (76%), *Mycobacterium smegmatis* (67%), *Mycobacterium gilvan* (67%), *Mycobacterium vanbaalenii* (65%), and *Mycobacterium abscessus* (64%), but not to *M. tuberculosis*, by BLASTP search (http://blast.ncbi.nlm.nih.gov/Blast.cgi). Two chaperons, *DnaK* and *GroEL*, were also highly expressed (third and fifth strongest, respectively).

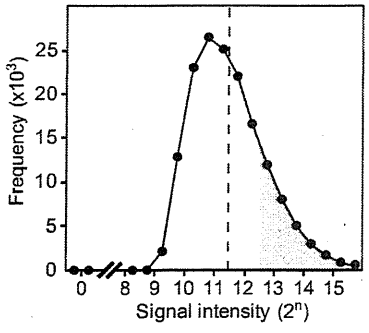

Fig. 1. Distribution of signal intensities detected using *Mycobacterium leprae* open reading frame (ORF) array. *M. leprae* ORF array was hybridized with RNA extracted from the Thai53 strain of *M. leprae*. Obtained signal intensities are shown as 2^n for each signal intensity. The median (2900) of the normalized entire signal intensities is indicated by a dashed line. The area whose signal intensity is twofold stronger than the median (*i.e.*, 5800 or $2^{12.5}$) is indicated by shading.

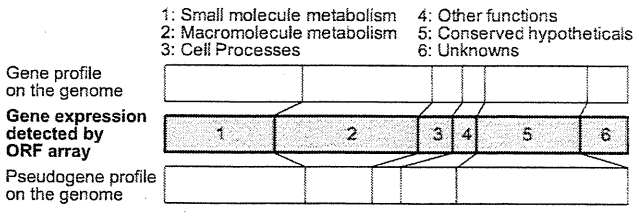

Fig. 2. Highly expressed gene within functional classes. Functional classes of highly expressed genes were compared with their original proportion in the genes and pseudogenes according to the classification by Cole et al. [7]. The significance of gene expression on each functional class was evaluated by the chi-square test ($\chi^2 = 1.0$, $p = 0.960$ for the genes and $\chi^2 = 23.4$, $p = 0.003$ for the pseudogenes).

Table 1
Functional classification of genes whose expression ratio was twofold higher than the median.

Classification	Number of genes expressed	Number of genes in the genome	Expression ratio (%)
I Small molecule metabolism			14.5
I.A Degradation	6	49	12.2
I.B Energy metabolism	18	91	19.8
I.C Central intermediary metabolism	8	30	26.7
I.D Amino acid biosynthesis	8	77	10.4
I.E Polyamine synthesis	0	0	0.0
I.F Purines, pyrimidines, nucleosides and nucleotides	11	52	21.2
I.G Biosynthesis of cofactors, prosthetic groups and carriers	6	63	9.5
I.H Lipid biosynthesis	5	35	14.3
I.I Polyketide and non-ribosomal peptide synthesis	2	13	15.4
I.J Broad regulatory functions	9	57	15.8
II Macromolecule metabolism			20.1
II.A Synthesis and modification of macromolecules	42	159	26.4
II.B Degradation of macromolecules	6	43	14.0
II.C Cell envelope	51	256	19.9
III Cell processes			27.3
III.A Transport/binding proteins	8	55	14.5
III.B Chaperones/heat shock	6	14	42.9
III.C Cell division	4	11	36.4
III.D Protein and peptide secretion	2	10	20.0
III.E Adaptations and atypical conditions	1	6	16.7
III.F Detoxification	2	6	33.3
IV Other[a]			21.5
IV.A Virulence	1	7	14.3
IV.B IS elements, repeated sequences, and phage	0	4	0.0
IV.C PE and PPE families	5	11	45.5
IV.D Antibiotic production and resistance	0	1	0.0
IV.E Bacteriocin-like proteins	0	0	0.0
IV.F Cytochrome P450 enzymes	1	1	100.0
IV.G Coenzyme F420-dependent enzymes	1	2	50.0
IV.H Miscellaneous transferases	7	35	20.0
IV.I Miscellaneous phosphatases, lyases, and hydrolases	1	15	6.7
IV.J Cyclases	0	0	0.0
IV.K Chelatases	0	0	0.0
V Conserved hypotheticals	71	360	19.7
VI Unknowns	33	141	23.4
Total	315	1604	19.6

[a] This class includes one gene that is not sub-classified.

Table 2
Genes with more than tenfold stronger expression than the median.

Fold of median	Acc. No.	Classification	Gene name
17.6	ML0065	I.B.7	Probable monooxygenase *EthA*
16.4	ML2313	VI	Hypothetical protein
15.6	ML2496	III.B	Molecular chaperone *DnaK*
15.1	ML2042	III.F	Alkyl hydroperoxide reductase
14.6	ML0317	III.B	Chaperonin *GroEL*
14.2	ML1735	I.F.3	Probable *NrdI*-family protein
13.7	ML1394	II.A.6	Translation initiation factor *IF-3*
13.1	ML0577	III.D	Probable preprotein translocase *SecA1* subunit
12.5	ML0319	II.C.1	Possible lipoprotein *LpqE*
11.4	ML0050	II.C.2	Possible 10 kDa culture filtrate antigen homolog *EsxB* (*lhp*) (*cfp10*)
11.0	ML2135	II.C.4	Possible transmembrane protein
10.3	ML1171	II.C.4	Possible conserved integral membrane protein

2.3. Detection of expressed operons in M. leprae genome

In the course of analyzing 315 highly expressed genes, we found some sequential expressions of gene sets. We therefore mapped highly expressed genes to the entire genome structure (http://www.sanger.ac.uk/Projects/M_leprae/) and detected 19 sequential regions that have three or more genes highly expressed in the same direction (Table 3). Of these 19 regions, seven were known operons reported in *M. leprae* or *M. tuberculosis* (Table 3, Nos. 1–7). These highly expressed operons include genes related to protein synthesis of ribosome subunits ML1132-ML1134 (*rho*, *rpmE* and *prfA*), ML1957-1962 (*rpoA*, *rpsD*, *rpsK*, *rpsM*, *rpmJ* and *infA*), and ML2683-ML2685 (*prsR*, *ssb* and *rpsF*) (Table 3, Nos. 3, 4, and 7, respectively). Also, 6-kDa early secreted antigenic target (ESAT-6) and culture filtrate protein 10 (CFP-10) family genes ML0049-ML0050 (*esxA* and *esxB*) and ML2531-ML2532 (*esxH* and *esxG*), which are known virulent factors of *M. tuberculosis* (Table 3, Nos. 1 and 6, respectively), were highly expressed within operons. Others include secretion in mycobacteria (*Snm*) proteins ML0406-ML0407 (*Snm9* and *Snm10*) (Table 3, No. 2) and molecular chaperons ML2494-ML2496 (*dnaJ*, *grpE* and *dnaK*) (Table 3, No. 5).

To predict possible operon structures in the consecutively expressed gene regions that were identified, three programs were used: MicrobesOnline (http://www.microbesonline.org/operons/gnc1769.html) [13], Operon DataBase (http://operondb.cbcb.umd.edu/cgi-bin/operondb/operons.cgi) [14], and DOOR (http://csbl1.bmb.uga.edu/OperonDB/index.php) [15]. By using these programs, six out of seven known operons were successfully predicted by two or all three programs. Among 12 operon candidates identified in this study (Table 3, Nos. 8–19), 11 were predicted as operon by two or all three programs and seven by all three programs. These potential operons include ABC transporter components (ML1425-ML1427) (Table 3, No. 13) that are expected to import carbohydrates [16] and *nrd* protein genes that catalyze *de novo* synthesis of deoxyribonucleotides [17] *nrdE*, *nrdI*, and *nrdH* (ML1734-ML1736) (Table 3, No. 16).

3. Discussion

We took advantage of *M. leprae* ORF array on which gene-specific multiple probes were arranged. By using highly purified *M. leprae* RNA from SHR/NCrj-*rnu* rats, where *M. leprae* notably proliferates and causes disease resembling that of humans [18,19], it was possible to analyze the gene expression profile of the entire range of *M. leprae* genes that may cause disease resembling that seen in humans.

Highly expressed genes were detected similarly from the six functional classes without significant deflection. Among these genes, five were related to Acyl-CoA metabolic enzymes. The metabolite of these enzymes, phthiocerol dimycocerosate (DIM) lipids, composes the cell wall of only pathogenic mycobacteria and this group of lipids is thought to play a role in cell wall architecture and permeability that affect virulence [20,21]. Because all the five genes detected in *M. leprae* have their corresponding orthologues in *M. tuberculosis*, these genes may play essential roles in the virulence of both species.

Table 3
Known and possible operons detected using ORF array.

No.	Genes expressed sequentially	Refs.	Functional class	Prediction programs		
				Microbes online[a]	Operon Database[b]	DOOR[c]
Known operons						
1	ML0048, ML0049, ML0050	[10]	V, II.C.2, II.C.2	–	+	+
2	ML0405, ML0406, ML0407	[16]	V, V, V	–	+	+
3	ML1132, ML1133, ML1134	[18]	II.A.7, II.A.1, II.A.6	–	+	–
4	ML1957, ML1958, ML1959, ML1960, ML1961, ML1962	[18]	II.A.7, II.A.1, II.A.1, II.A.1, II.A.1, II.A.6	+	+	+
5	ML2494, ML2495, ML2496	[33]	III.B, III.B, III.B	+	+	+
6	ML2530, ML2531, ML2532	[17]	I.J.1, II.C.2, IV.C.1.a	–	+	+
7	ML2683, ML2684, ML2685	[18]	II.A.1, II.A.5, II.A.1	+	+	+
Novel operon candidates						
8	ML0125, ML0126, ML0127	None	IV.H, VI, VI	–	+	–
9	ML0245, ML0246, ML0247	None	II.A.1, II.C.1, III.F	–	+	+
10	ML0574, ML0575, ML0576, ML0577, ML0578	None	VI, VI, VI, III.D, I.C.1	–	+	+
11	ML0592, ML0593, ML0594	None	I.J.1, V, V	+	+	+
12	ML1180, ML1181, ML1182	None	V, V, IV.C.2	–	+	+
13	ML1425, ML1426, ML1427	None	III.A.3, III.A.3, III.A.3	+	+	+
14	ML1468, ML1469, ML1470	None	II.B.1, I.F.5, II.C.4	+	+	+
15	ML1616, ML1617, ML1618	None	II.A.2, V, II.A.1	+	+	+
16	ML1734, ML1735, ML1736	None	I.F.3, I.F.3, I.F.3	+	+	+
17	ML1905, ML1906, ML1907	None	II.A.1, II.A.7, III.D	+	+	+
18	ML2259, ML2260, ML2261	None	II.C.4, III.A.4, V	–	+	+
19	ML2706, ML2707, ML2708, ML2709	None	III.C, III.C, V, V	+	+	+

–: no prediction, +: predicted.
[a] MicrobesOnline (http://www.microbesonline.org/operons/gnc1769.html) [13].
[b] Operon DB (http://operondb.cbcb.umd.edu/cgi-bin/operondb/operons.cgi) [14].
[c] DOOR (http://csbl1.bmb.uga.edu/OperonDB/index.php) [15].

Molecular chaperons were also strongly expressed in *M. leprae*, which may be associated with the strong host immune response against these chaperones, such as HSP70, as previously reported [22,23]. Putative monooxygenase (ML0065), an orthologue of *M. tuberculosis* flavin monooxygenase *EthA*, which is reported to be an activator of thiocarbamide-containing antibiotics [24,25], was also strongly expressed. Since *katG*, another activator enzyme of thiocarbamide-containing antibiotics in *M. tuberculosis* [26], is a pseudogene in *M. leprae* [27], the role of *EthA* in *M. leprae* might be more important. Our BLASTP search revealed that ML2313, which showed the second strongest expression and contained no orthologue in the *M. tuberculosis* genome, was homologous to the transcription regulator *padR*. Specifically, *padR* is a negative regulator of phenolic acid decarboxylases *padA* and *padC*, both of which catalyze phenolic acid antibiotics to their vinyl derivatives [28]. Thus, the present analysis of *M. leprae* gene expression provides interesting possibilities of gene function and suggests a distinctive feature of *M. leprae* genes that might be related to the sensitivity to certain drugs. We have also tried to identify genes whose expression was as low as background. Although many hypothetical proteins were included in this group, further analysis will be necessary to elucidate suppressed genes by comparing gene expression of *M. leprae* infected in susceptible and non-susceptible hosts.

In prokaryotes, functionally related genes are transcribed in a single RNA strand forming an operon, and RNA expression from operons has been reported in *M. leprae* and *M. tuberculosis*. These operons include ribosome components [29,30] and genes involved in carbohydrate transport [31], which are essential for homeostasis, as well as genes related to virulence, such as entry operon (*mce*) [32], ESAT-6 and CFP-10 family secreted proteins [33], and heat shock proteins [5]. In the present study, we identified seven known operons and 11 novel putative operons, which included ribosomal proteins, ESAT-6 and CFP-10 family proteins, Snm proteins, and molecular chaperones. Ribosomal proteins are clustered in highly conserved operons which are preserved among prokaryotes including *M. leprae* [30] in order to function collectively as parts of a complex molecular machinery of the ribosome. ESAT-6 and CFP-10 family proteins are limited only to *Mycobacterium* species and play an important role in *Mycobacterium* virulence and host immune response [33–35]. Their distantly related protein, Snm, is thought as a component of the secretion system for ESAT-6 and CFP-10 family together with other proteins [36]. The multiple expressions of these mutually related gene groups as operons imply their involvement in the intracellular survival strategies and virulence of *M. leprae*.

Among the newly identified operon candidates, nucleotide reduction gene (*nrd*) operon (ML1734-ML1736) has been reported in other bacteria but never in *Mycobacterium* [17]. Further analysis of their promoter regions will determine the precise range of these putative operons.

In summary, we have analyzed *M. leprae* gene expression profile using DNA microarray and identified highly expressed genes and novel operon candidates. These data will serve as a basis for further investigation of the function of *M. leprae* genes in relation to its unique characteristics, such as long-term latency, inability to grow *in vitro*, and high proportion of pseudogenes.

4. Materials and methods

4.1. Bacterial strains and growth conditions

Hypertensive nude rats (SHR/NCrj-*rnu*), in which the Thai53 strain of *M. leprae* was actively grown [18,19], were kindly provided by Dr. Y. Yogi of the Leprosy Research Center, National Institute of Infectious Diseases, Japan. *M. leprae* was isolated as previously described [10]. Briefly, the footpads of the SHR/NCrj-*rnu* rats were homogenized in Hank's balanced salt solution (HBSS) containing 0.025% Tween 80. The sample was centrifuged at 700g and 4 °C for 10 min to remove tissue debris. The supernatant was treated with 0.5% trypsin at 37 °C for 1 h, followed by centrifugation at 5000g and 4 °C for 20 min. The pellet was resuspended in 10 ml of HBSS containing 0.025% Tween 80 and 0.25 N NaOH. Further incubation at 37 °C for 15 min was followed by centrifugation, then the pellet was resuspended in 2 ml of phosphate buffered saline (PBS). Two microliters of the solution was spread on a glass slide and subjected to acid fast staining to count the number of bacilli.

4.2. RNA extraction from M. leprae

M. leprae RNA was prepared as described [10,11]. Briefly, bacilli (2.8×10^{11} cells) were suspended in 2 ml of RNA Protect Bacteria Reagent (QIAGEN, Germantown, MD) and vortexed. After standing for 10 min at room temperature, the cells were collected and treated in another 2 ml of the same reagent; to this bacilli-containing mixture, 0.4 ml of 1.0 mm Zirconia Beads (BioSpec Products, Bartlesville, OK) and 0.6 ml of Lysis/Binding buffer, a component of the mirVana miRNA Isolation kit (Ambion, Austin, TX), were added. The mixture was homogenized at 3000 rpm for 3 min using a Micro Smash (TOMY, Tokyo Japan) followed by four freeze–thaw cycles. RNA was extracted according to the manufacturer's instructions (Ambion). The extracted RNA was treated with DNase I (TaKaRa, Kyoto Japan).

4.3. Array design and analysis

ORF array from NimbleGen Systems (Madison, WI) was used for array analysis. In this array, 20 different highly specific 60 mer probes designed for each of the 1605 ORFs were mounted with multiple control probes. Probes were designed based on the sequence and CDS information from Sanger Institute (http://www.sanger.ac.uk/Projects/M_leprae/). These probes were arranged into five blocks on a glass plate. As a result, a total of 160,500 probes were used to analyze RNA expression from *M. leprae* ORF. Twenty micrograms of total RNA from *M. leprae* was reverse-transcribed using SuperScript II (Invitrogen, Carlsbad, CA). The generated cDNA was incubated with 10 ng of RNase A (Novagen, Madison, WI) at 37 °C for 10 min, phenol-chloroform extracted, and precipitated with ethanol. For Cy3 labeling, 1 μg of ds-cDNA was incubated with 1 OD_{600} unit of Cy3-9mer Wobble primer (TriLink Biotechnologies, San Diego, CA) for 10 min at 98 °C. Then, 8 mmol dNTPs and 100 U of Klenow fragment (New England Biolabs, Ipswich, MA) were added, followed by incubation at 37 °C for 2 h. The reaction was stopped by adding 0.1 volume of 0.5 M EDTA, and the labeled cDNA was precipitated with isopropanol. Array analysis was performed as previously described [10].

Acknowledgements

The authors wish to thank D.B. Pham, M. Hayashi, K. Nakamura, M. Sue, Y. Ishido, and S. Sekimura (LRC, NIID) for useful discussions. This work was supported by a Grant-in-Aid for Scientific Research on Priority Areas from the Ministry of Education, Culture, Sports, Science, and Technology of Japan (K.S.), Japan Health Sciences Foundation (T.A.), and by a Grant-in-Aid for Research on Emerging and Reemerging Infectious Diseases from the Ministry of Health, Labour, and Welfare of Japan (N.I.).

Appendix. Supplementary data

Supplementary data associated with this article can be found in the online version, at doi:10.1016/j.micpath.2010.05.010.

References

[1] Engers H, Morel CM. Leprosy. Nat Rev Microbiol 2003;1:94–5.
[2] Barker LP. *Mycobacterium leprae* interactions with the host cell: recent advances. Indian J Med Res 2006;123:748–59.
[3] Curtiss 3rd R, Blower S, Cooper K, Russell D, Silverstein S, Young L. Leprosy research in the post-genome era. Lepr Rev 2001;72:8–22.
[4] Agrawal VP, Shetty VP. Comparison of radiorespirometric Budemeyer assay with ATP assay and mouse foot pad test in detecting viable *Mycobacterium leprae* from clinical samples. Indian J Med Microbiol 2007;25:358–63.
[5] Williams DL, Pittman TL, Deshotel M, Oby-Robinson S, Smith I, Husson R. Molecular basis of the defective heat stress response in *Mycobacterium leprae*. J Bacteriol 2007;189:8818–27.
[6] Wieles B, Ottenhoff TH, Steenwijk TM, Franken KL, de Vries RR, Langermans JA. Increased intracellular survival of *Mycobacterium smegmatis* containing the *Mycobacterium leprae* thioredoxin–thioredoxin reductase gene. Infect Immun 1997;65:2537–41.
[7] Cole ST, Eiglmeier K, Parkhill J, James KD, Thomson NR, Wheeler PR, et al. Massive gene decay in the leprosy bacillus. Nature 2001;409:1007–11.
[8] Monot M, Honore N, Garnier T, Zidane N, Sherafi D, Paniz-Mondolfi A, et al. Comparative genomic and phylogeographic analysis of *Mycobacterium leprae*. Nat Genet 2009;41:1282–9.
[9] Gutierrez MC, Supply P, Brosch R. Pathogenomics of mycobacteria. Genome Dyn 2009;6:198–210.
[10] Akama T, Suzuki K, Tanigawa K, Kawashima A, Wu H, Nakata N, et al. Whole-genome tiling array analysis of *Mycobacterium leprae* RNA reveals high expression of pseudogenes and noncoding regions. J Bacteriol 2009;191:3321–7.
[11] Suzuki K, Nakata N, Bang PD, Ishii N, Makino M. High-level expression of pseudogenes in *Mycobacterium leprae*. FEMS Microbiol Lett 2006;259:208–14.
[12] Williams DL, Torrero M, Wheeler PR, Truman RW, Yoder M, Morrison N, et al. Biological implications of *Mycobacterium leprae* gene expression during infection. J Mol Microbiol Biotechnol 2004;8:58–72.
[13] Price MN, Huang KH, Alm EJ, Arkin AP. A novel method for accurate operon predictions in all sequenced prokaryotes. Nucleic Acids Res 2005;33:880–92.
[14] Pertea M, Ayanbule K, Smedinghoff M, Salzberg SL. OperonDB: a comprehensive database of predicted operons in microbial genomes. Nucleic Acids Res 2009;37:D479–82.
[15] Mao F, Dam P, Chou J, Olman V, Xu Y. DOOR: a database for prokaryotic operons. Nucleic Acids Res 2009;37:D459–63.
[16] Titgemeyer F, Amon J, Parche S, Mahfoud M, Bail J, Schlicht M, et al. A genomic view of sugar transport in *Mycobacterium smegmatis* and *Mycobacterium tuberculosis*. J Bacteriol 2007;189:5903–15.
[17] Jacobson BA, Fuchs JA. Multiple cis-acting sites positively regulate *Escherichia coli nrd* expression. Mol Microbiol 1998;28:1315–22.
[18] Yogi Y, Banba T, Kobayashi M, Katoh H, Jahan N, Endoh M, et al. Leprosy in hypertensive nude rats (SHR/NCrj-*rnu*). Int J Lepr Other Mycobact Dis 1999;67:435–45.
[19] Yogi Y, Endoh M, Banba T, Kobayashi M, Katoh H, Suzuki K, et al. Susceptibility to *Mycobacterium leprae* of congenic hypertensive nude rat (SHR/NCrj-*rnu*) and production of cytokine from the resident peritoneal macrophages. Jpn J Lep 2002;71:39–45.
[20] Camacho LR, Constant P, Raynaud C, Laneelle MA, Triccas JA, Gicquel B, et al. Analysis of the phthiocerol dimycocerosate locus of *Mycobacterium tuberculosis*. Evidence that this lipid is involved in the cell wall permeability barrier. J Biol Chem 2001;276:19845–21954.
[21] Goyal A, Yousuf M, Rajakumara E, Arora P, Gokhale RS, Sankaranarayanan R. Crystallization and preliminary X-ray crystallographic studies of the N-terminal domain of FadD28, a fatty-acyl AMP ligase from *Mycobacterium tuberculosis*. Acta Crystallogr Sect F Struct Biol Cryst Commun 2006;62:350–2.
[22] Oftung F, Lundin KE. Identification of *Mycobacterial* HSP70 reactive human T cell clones discriminating between *M. tuberculosis* and *M. leprae*. FEMS Immunol Med Microbiol 1998;20:145–51.
[23] Roche PW, Peake PW, Davenport MP, Britton WJ. Identification of a *Mycobacterium leprae*-specific T cell epitope on the 70 kDa heat shock protein. Immunol Cell Biol 1994;72:215–21.
[24] Dover LG, Alahari A, Gratraud P, Gomes JM, Bhowruth V, Reynolds RC, et al. EthA, a common activator of thiocarbamide-containing drugs acting on different mycobacterial targets. Antimicrob Agents Chemother 2007;51:1055–63.
[25] Qian L, Ortiz de Montellano PR. Oxidative activation of thiacetazone by the *Mycobacterium tuberculosis* flavin monooxygenase EtaA and human FMO1 and FMO3. Chem Res Toxicol 2006;19:443–9.
[26] Morlock GP, Metchock B, Sikes D, Crawford JT, Cooksey RC. *ethA, inhA*, and *katG* loci of ethionamide-resistant clinical *Mycobacterium tuberculosis* isolates. Antimicrob Agents Chemother 2003;47:3799–805.
[27] Nakata N, Matsuoka M, Kashiwabara Y, Okada N, Sasakawa C. Nucleotide sequence of the *Mycobacterium leprae katG* region. J Bacteriol 1997;179:3053–7.
[28] Licandro-Seraut H, Gury J, Tran NP, Barthelmebs L, Cavin JF. Kinetics and intensity of the expression of genes involved in the stress response tightly induced by phenolic acids in *Lactobacillus plantarum*. J Mol Microbiol Biotechnol 2008;14:41–7.
[29] Gonzalez-y-Merchand JA, Colston MJ, Cox RA. The rRNA operons of *Mycobacterium smegmatis* and *Mycobacterium tuberculosis*: comparison of promoter elements and of neighbouring upstream genes. Microbiology 1996;142(Pt 3):667–74.
[30] Makarova KS, Ponomarev VA, Koonin EV. Two C or not two C: recurrent disruption of Zn-ribbons, gene duplication, lineage-specific gene loss, and horizontal gene transfer in evolution of bacterial ribosomal proteins. Genome Biol 2001;2. RESEARCH 0033.
[31] Borich SM, Murray A, Gormley E. Genomic arrangement of a putative operon involved in maltose transport in the *Mycobacterium tuberculosis* complex and *Mycobacterium leprae*. Microbios 2000;102:7–15.
[32] Wiker HG, Spierings E, Kolkman MA, Ottenhoff TH, Harboe M. The mammalian cell entry operon 1 (*mce1*) of *Mycobacterium leprae* and *Mycobacterium tuberculosis*. Microb Pathog 1999;27:173–7.
[33] Geluk A, van Meijgaarden KE, Franken KL, Subronto YW, Wieles B, Arend SM, et al. Identification and characterization of the ESAT-6 homologue of *Mycobacterium leprae* and T-cell cross-reactivity with *Mycobacterium tuberculosis*. Infect Immun 2002;70:2544–8.
[34] Maciag A, Dainese E, Rodriguez GM, Milano A, Provvedi R, Pasca MR, et al. Global analysis of the *Mycobacterium tuberculosis* Zur (FurB) regulon. J Bacteriol 2007;189:730–40.
[35] Spencer JS, Kim HJ, Marques AM, Gonzalez-Juarerro M, Lima MC, Vissa VD, et al. Comparative analysis of B- and T-cell epitopes of *Mycobacterium leprae* and *Mycobacterium tuberculosis* culture filtrate protein 10. Infect Immun 2004;72:3161–70.
[36] MacGurn JA, Raghavan S, Stanley SA, Cox JS. A non-RD1 gene cluster is required for Snm secretion in *Mycobacterium tuberculosis*. Mol Microbiol 2005;57:1653–63.

OPEN ACCESS Freely available online

PLoS one

Detection of *Mycobacterium leprae* DNA from Archaeological Skeletal Remains in Japan Using Whole Genome Amplification and Polymerase Chain Reaction

Koichi Suzuki[1]*, Wataru Takigawa[2], Kazunari Tanigawa[1], Kazuaki Nakamura[3], Yuko Ishido[1], Akira Kawashima[1], Huhehasi Wu[1], Takeshi Akama[1], Mariko Sue[1], Aya Yoshihara[1], Shuichi Mori[4], Norihisa Ishii[5]

1 Laboratory of Molecular Diagnostics, Department of Mycobacteriology, Leprosy Research Center, National Institute of Infectious Diseases, Tokyo, Japan, **2** School of Rehabilitation Sciences at Fukuoka, International University of Health and Welfare, Fukuoka, Japan, **3** Department of Pharmacology, National Research Institute for Child Health and Development, Tokyo, Japan, **4** Laboratory of Molecular Epidemiology and Social Science, Leprosy Research Center, National Institute of Infectious Diseases, Tokyo, Japan, **5** Leprosy Research Center, National Institute of Infectious Diseases, Tokyo, Japan

Abstract

Background: Identification of pathogen DNA from archaeological human remains is a powerful tool in demonstrating that the infectious disease existed in the past. However, it is very difficult to detect trace amounts of DNA remnants attached to the human skeleton, especially from those buried in a humid atmosphere with a relatively high environmental temperature such as in Asia.

Methodology/Principal Findings: Here we demonstrate *Mycobacterium leprae* DNA from archaeological skeletal remains in Japan by polymerase chain reaction, DNA sequencing and single nucleotide polymorphism (SNP) analysis. In addition, we have established a highly sensitive method of detecting DNA using a combination of whole genome amplification and polymerase chain reaction, or WGA-PCR, which provides superior sensitivity and specificity in detecting DNA from trace amounts of skeletal materials.

Conclusion/Significance: We have detected *M. leprae* DNA in archaeological skeletal remains for the first time in the Far East. Its SNP genotype corresponded to type 1; the first detected case worldwide of ancient *M. leprae* DNA. We also developed a highly sensitive method to detect ancient DNA by utilizing whole genome amplification.

Citation: Suzuki K, Takigawa W, Tanigawa K, Nakamura K, Ishido Y, et al. (2010) Detection of *Mycobacterium leprae* DNA from Archaeological Skeletal Remains in Japan Using Whole Genome Amplification and Polymerase Chain Reaction. PLoS ONE 5(8): e12422. doi:10.1371/journal.pone.0012422

Editor: Immo A. Hansen, New Mexico State University, United States of America

Received April 18, 2010; **Accepted** August 4, 2010; **Published** August 26, 2010

Funding: This work was supported by Grant-in-Aid for Research on Emerging and Re-emerging Infectious Diseases from the Ministry of Health, Labour, and Welfare of Japan. The funders had no role in study design, data collection and analysis, decision to publish, or preparation of the manuscript.

Competing Interests: The authors have declared that no competing interests exist.

* E-mail: koichis@nih.go.jp

Introduction

Leprosy is a chronic infectious disease caused by *Mycobacterium leprae* (*M. leprae*) and has affected humans for millennia. Whole genome sequence analysis of *M. leprae* has revealed that the genome is 3.3 Mbp in size, with only 1,605 genes that encode proteins and 1,115 pseudogenes [1]. Trough comparative genome analysis of *M. leprae* strains from Brazil, India, Thailand and United States, remarkably little genomic diversity has been uncovered suggesting that leprosy has a single clonal origin [2,3]. Phylogeographic analysis of single nucleotide polymorphisms (SNPs) has revealed that *M. leprae* originated in Africa and spread to European and Asian countries and then worldwide along with human migrations and trade routes. Such geographic and temporal migration has also been demonstrated by SNPs analysis of ancient *M. leprae* DNA present in skeletal remains as old as 1,500 years ago [2,3].

Leprosy results in multiple deformities including progressive bone defects secondary to the peripheral neuropathy caused by *M. leprae* infection [4,5]. Additionally, in advanced cases *M. leprae* infection causes specific osteological deformations in the areas of the nasal aperture, anterior nasal spine and alveolar process on the premaxilla, cortical areas of the tibia and fibula, distal ends of the metatarsals and diaphyses of the phalanges that may include both direct and reactive changes [6,7,8,9,10]. Paleopathological diagnosis of leprosy has been made solely based on these macroscopic changes in skeletal remnants. However, it is occasionally difficult to make a definitive paleopathological diagnosis of leprosy solely based on osseous lesions, because syphilis, tuberculosis and other infectious and granulomatous diseases as well as carcinomas of nasal or oral origin will cause rhinomaxillary lesions similar to leprosy.

Direct detection of DNA remnants of pathogenic microorganisms from ancient human skeletons using polymerase chain reaction (PCR) is becoming a powerful molecular tool for clearly demonstrating the presence of pathogens within the skeletal remains [11]. This method provides an inestimable tool for investigating the temporal and geographical spread of infectious

diseases in human history, in addition to the anthropological interest in diagnosing infectious diseases in ancient remains. By the use of so-called palaeomicrobiology, it may be possible to elucidate the epidemiology of past infectious disease by reconstituting the distribution of infected individuals, which is especially important in the field of emergence and re-emergence of infectious diseases [11]. Moreover, it may also be possible to track the genetic evolution of the pathogenic microorganisms.

A study employing paleomicrobiology was first reported in 1993, demonstrating the presence of *Mycobacterium tuberculosis* (*M. tuberculosis*) DNA using PCR from an ancient human skeleton [12]. Detection of *M. leprae* DNA was reported the next year [13] from ancient bone dating from 600 AD, followed closely by several other reports [14,15,16,17,18,19,20,21]. However, all of these studies used European and Middle Eastern archaeological materials from countries such as England, Germany, Denmark, Poland, Hungary, Czech, Croatia, Turkey, Israel and Egypt, but not from the Far East Asian countries. This may be related to the superior preservation of ancient buried skeletons in these countries compared to that in more a humid atmosphere with a relatively high environmental temperature, such as is commonly found in Asia [22].

Recently, we have obtained permission to examine skeletal remains excavated in Japan with paleopathological evidence of leprosy In the present study, we demonstrate *M. leprae* DNA and SNPs from skeletal remains. We also describe a highly sensitive whole genome amplification (WGA)-PCR method that may be suitable for detecting trace amounts of ancient microbial DNA.

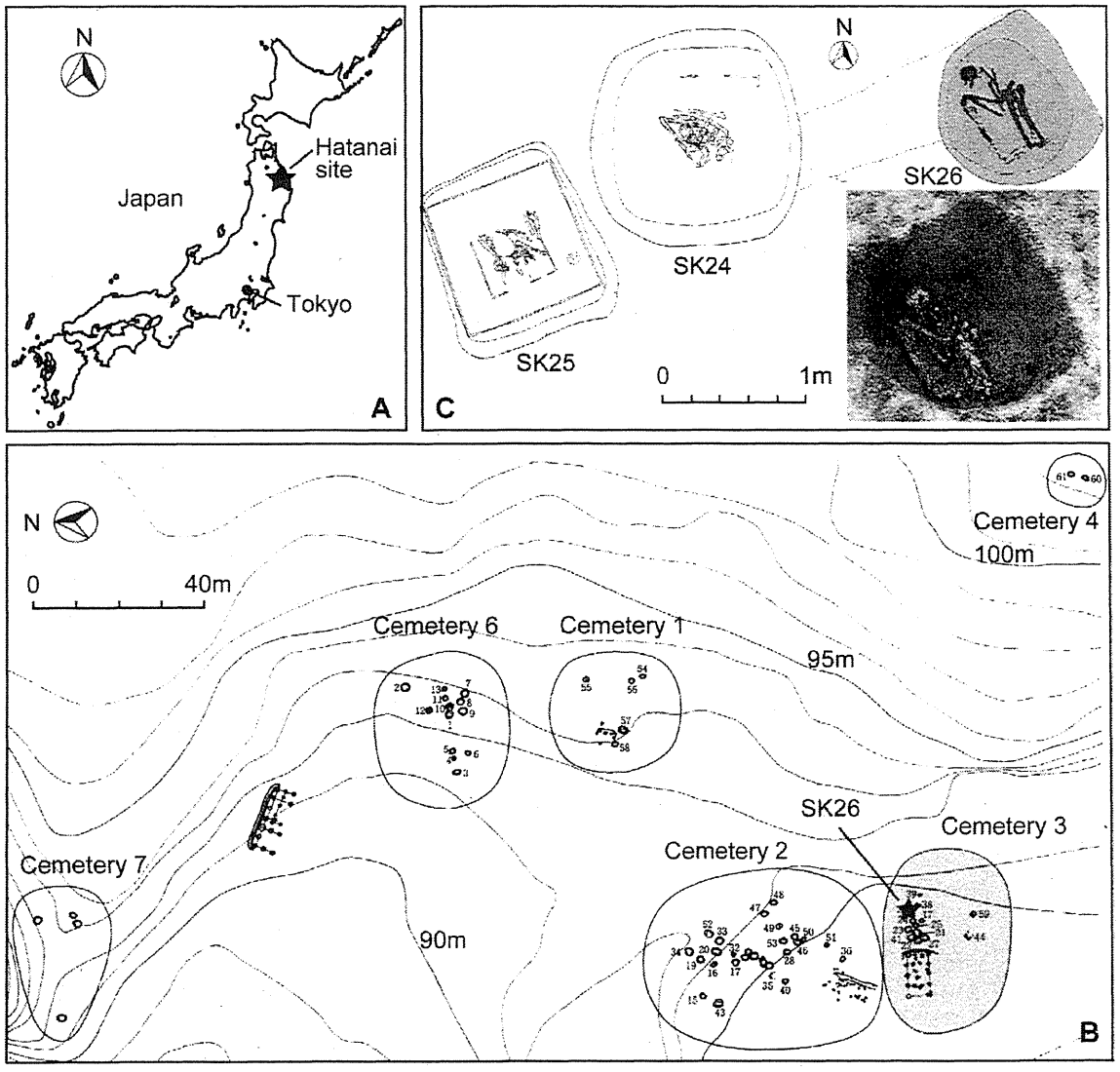

Figure 1. Geographical representation of excavation site. Location of *Hatanai* site in northeastern Japan (A). A map of seven cemeteries and the site where SK26 was excavated (B). A grave pit of SK26 at excavated (C) Cemetery 5 (not shown in this map) locates 50 m south of cemetery 2. All these figures were modified with permission from reference [23].
doi:10.1371/journal.pone.0012422.g001

Materials and Methods

Archaeological background and osteological description

The materials used in this study were archaeological skeletal remains excavated from the *Hatanai* site (N40°22′, E141°29′) in Aomori prefecture, in the northeastern part of Honshu Island in Japan (Fig. 1A). The *Hatanai* site consists of several strata including artifacts and remnants from the prehistoric Initial-Middle Jomon (ca. 8000-4500 BP) to pre-modern Edo period (1603–1867). All skeletal materials are stored in the Tohoku University Museum, Sendai, Japan.

The present material (Grave No. SK26) was buried at a gravel pit of an Edo-period cemetery in a farm village, in which was found about 50 human skeletal remains (Fig. 1B). This corpse was lying on its left side and hunching its back, with the elbow, hip and knee joints closely flexed inside the burial pit (Fig. 1C). It is not clear whether or not SK26 was placed in a wooden coffin. The SK26 skeleton had only one *Kouki-tsuhou (Kangxi-tongbao)*, a metallic currency used during the rule of the Emperor Kangxi (reign in 1661–1722) of the Qing dynasty (1616–1912) in China, as grave goods. Accordingly, the age of this burial is estimated as the middle 18th to the early 19th century, as supposed by evidences from other graves [23].

SK26's skull was almost perfectly intact except for part of the cranial base and parietal bones (Fig. 2). Although its main long bones were intact, many of their epiphyses and all the hand/foot bones were missing within the burial matrix of the postmortem environment. The sex of this skeleton was assessed as male on the basis of cranial morphologies, such as anterior decline of the frontal bone, projection of the superciliary ridge, inferior prominence of the mastoids, and developments of the superior nuchal line and the external occipital protuberance. But its bilateral pelvis was incompletely preserved and therefore unavailable for sex and age determination.

The age at death was estimated from dental attrition and fusions of the cranial sutures. Surviving permanent teeth were worn to dentine, including the 3rd molar. In the calvarium, the unions of all sutures in the internal table were finished; coronal and lambdoid sutures of the external table had incomplete fusing. These dental and skeletal evidences suggest that of the age of death, SK26 was middle-aged, in the range of 30–50 years old.

Palaeopathological observations and diagnosis

The facial cranium of SK26 showed several typical symptoms of leprosy, suggestive of lepromatous type. In the rhinomaxillary area, rounding deformation and abnormal enlargement of the nasal aperture, disappearance of the anterior nasal spine, and severe atrophy of the alveolar process were clearly observed (Fig. 2). The palatal process showed degenerative changes, and alveolar bones at the anterior teeth were closed by antemortem loss of all upper incisors and the right canine. The incisor foramen in the hard palate had also disappeared due to osseous resorption; for maxillary atrophy, the vertical thickness of the palatal bone was about nine millimeters on the right side of the alveolar process, and at the same portion on the left, only six millimeters at the maximum value.

These features of craniofacial malformation, especially the rhinomaxillary syndrome, are specific to lepromatous leprosy but essentially distinct from other facial-deforming diseases such as craniofacial tuberculosis and syphilis, a treponematoses [7,8]. Although the nasal, maxillary and palatal lesions in craniofacial tuberculosis closely resemble those in lepromatous leprosy, cranial involvements of tuberculosis are extremely rare in adult patients and mainly appear in young children, often with lesions of the mandible. In tertiary syphilis, rhinomaxillary deformations accompany several

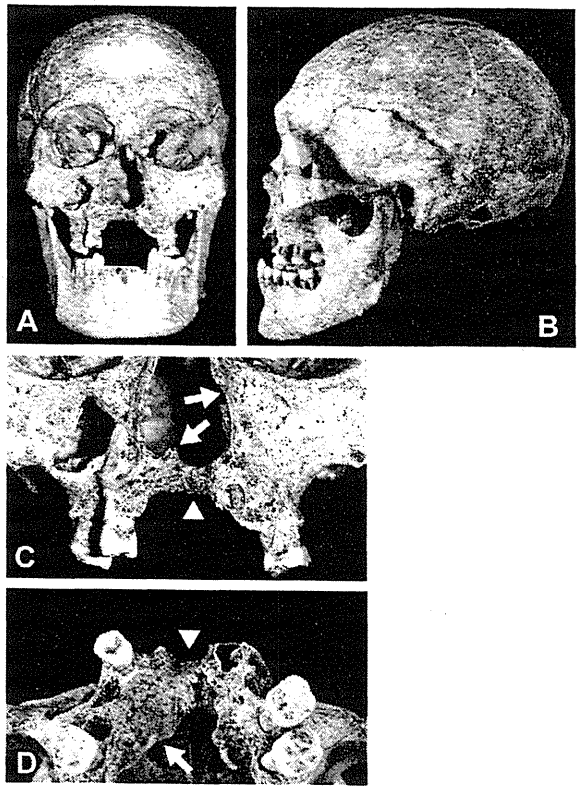

Figure 2. Macroscopic view of the skeletal lesion in the skull of sample SK26. Frontal view (A) and left side view (B) of the skull. Closer view of the nasal aperture and maxillary palate (C) and upward view of the palate (D). Arrows in panel C indicate erosive deformity of the nasal aperture and disappearance of the anterior nasal spine. Arrowheads in panels C and D indicate severe atrophy of alveolar bone in the maxilla/palatal process with loss of anterior teeth. An arrow in panel D denotes the locus of sample No. 1 shown in Table 1 and Figure 2.
doi:10.1371/journal.pone.0012422.g002

osteo-periostitic lesions and focal destructive remodeling (caries sicca) caused by the bone gummas in the cranial vault [7,8]. From differences in these pathological features, the facial deformities of SK26 were diagnosed as leprous symptoms.

In the bilateral tibiae and fibulae of this skeleton, slight periostitic changes were seen on the cortical surfaces of the diaphyses. The SK26 skeleton had lost its hand and foot bones from the long-term burial conditions, making it impossible to confirm any pencil-shaped recessions in the distal ends of the metacarpals, metatarsals or phalanges, which are typical leprous lesions.

Sampling of skeletal remains

Sampling was performed at the Tohoku University Museum, where no other leprous materials were stored. Skeletal samples were taken from the affected area as summarized in Table 1 using a small-sized rotating electric saw (Mini router, Kiso Power Tool, Osaka, Japan). Two samples were also taken from another skeleton (SK20; middle-aged male) found in the same cemetery, which had no leprous changes as a negative control for DNA purification and PCR analysis. One premolar root was extracted from another skeleton (SK16; middle-aged female) as a positive control for human DNA recovery. Sterile materials were used for the sampling to avoid possible contamination. Ethical

Table 1. Skeletal samples.

No.	Material reference	Sampling site	Paleopathological evidence	Sample weight (mg)
1	SK26	Maxillary palate, right	Erosion/atrophy	9.7
2	SK26	Inner surface of nasal cavity, right	Erosion/atrophy	6.0
3	SK26	Maxillary palate, left	Erosion/atrophy	4.6
4	SK26	Fibular diaphysis, right	Periostitis	22.1
5	SK20	Maxillary palate, right	N.R.	4.5
6	SK20	Inner surface of nasal cavity, right	N.R.	6.8
7	SK16	Lower 1st premolar root, right	N.R.	3.4

N.R.: No remarkable change.
doi:10.1371/journal.pone.0012422.t001

Table 2. PCR primer sequences.

Gene name	Synonym[a)]	Forward (5′-3′)	Reverse (5′-3′)	Length (bp)
Nested primer				
hsp-70, 1st	ML2496	gggctgtccaaggaagag	cgtcaaccacatcgtcagtag	391
(dnaK) 2nd		tcgtcaaggaacaacggg	cgtcaaccacatcgtcagtaga	261
16S rRNA, 1st	MLP000016	agagtttgatcctggctcag	tgcacacaggccacaaggga	1039
(*rrs*) 2nd		cggaaaggtctctaaaaaatctt	catcctgcaccgcaaaaagctt	171
SNP1, 1st	14,676	atttccaggtcttgtgcg	aggtcttcccaggacacc	351
2nd		aatggaatgctggtgagagc	caatgcatgctagccttaatga	194
SNP2, 1st	1,642,875	ttagtcaacatcgttagcagccc	actcataagcacggtgtctttgc	403
2nd		tgctagtttaaccgagtactgcta	gtagtagtcttccaagttgtggtg	189
SNP3, 1st	2,935,685	cgagcataatcgtaggcg	aaatgtggtcacctgggc	510
2nd		atctggtccgggtaggaatc	accggtgagcgcactaag	180
Gene				
cspA	ML0198	gaactgtgaagtggttcaacg	agcgaactccagtggcttg	186
hisE	ML1309	gaccttcgaggatctgttcg	atagacgtcatcgagcgaca	247
purM	ML2205	aaactcacgtccgtaccttc	agcacggtcagtatcttcag	233
cpsA	ML2247	ggcaccttcaccaacctaga	ccaacttaggatccgcttga	511
Pseudogene				
pseudo scoB	ML0434	tggaacacctcgtcgtatgtgg	tataagtggcaccgccgaactc	201
pseudo speE	ML0476	tcgcaacttcactgatcgtc	gtctggcaccaataccgagt	465
pseudo REP	ML0794	aaagacggagactacgatg	gtttagaaggttggtcgttg	191
pseudo ahpD	ML2043	tcaacatggcgatctgcattc	tgcgtgaccttacaacgct	200
Non-coding region				
	348,457	tggactcgatgttgaagtg	tgcttagctatgcagtgag	202
	1,593,211	catcgagtccaagctcaac	tgccgatgattacatcatcc	191
	2,134,972	cggaatcctgttgacgtgtt	cggcgctaacaactatcctc	242
	2,152,288	ccgatatgttcggtagtcgt	gcatcgatatcgccttcag	241
	2,307,322	ggttcaccggaagagttgg	cgcgacgactaagccagtag	242
	2,546,884	tcaatatggcttcctatgttgc	gctgcattaatccatgattcg	202
	2,551,060	acattcgagaccagctaccg	ttccgcttggaggataattg	194
	2,664,658	tgagcttgccgattacgatt	gccattgaactggccatc	227
	2,858,681	atgttggttgagcttggac	ttgcttagctatgcagtgag	217

Numbers in SNP nested primer indicate the coordinate location of the SNP. Numbers in non-coding regions indicate coordinate position of the primer within *M. leprae* genome (http://genolist.pasteur.fr/Leproma/).
doi:10.1371/journal.pone.0012422.t002

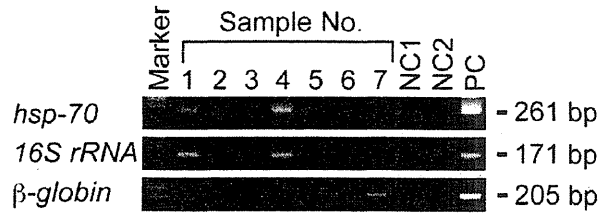

Figure 3. PCR detection of *M. leprae* DNA from skeletal samples. PCR analysis was performed using *M. leprae*-specific *hsp-70* and *16S-rRNA* primers for the DNA samples listed in Table 1. PCR products were evaluated by 2% agarose gel electrophoresis. Human *β-globin* gene was also PCR amplified as a control for DNA preparation from a premolar root. NC1: a negative control for DNA purification in which DNase/RNase-free water was used as a sample for DNA extraction; NC2: a negative control for PCR in which DNase/RNase-free water was used instead of a DNA sample for PCR reaction; and PC: positive control DNA from *Thai 53* strain of *M. leprae*.
doi:10.1371/journal.pone.0012422.g003

approval to work with the material was obtained from the review board at National Institute of Infectious Diseases, Japan. A permission to obtain the sample materials was granted by Tohoku University.

DNA preparations

DNA was purified using a QIAamp DNA Micro Kit (Qiagen, Valencia, CA) according to the manufacturer's protocol with some modification. Briefly, 500 µl of Buffer ATL was added to the skeletal samples placed in a 2 ml test tube. The tube was then filled with 1.0 mm diameter Zicronia beads (Bio Space Products, Inc, South Lancaster, MA) and homogenized using Micro Smash MS-100 (TOMY, Tokyo, Japan) at 3,000 rpm for 5 min at 4°C [24,25]. Samples were then frozen at −80°C, thawed at 37°C and homogenized for five times. The supernatant was subsequently treated with 40 µl of Proteinase K (20 mg/ml) and incubated overnight at 56°C. The samples were frozen and thawed, vortexed in 400 µl of Buffer AL then 400 µl of ethanol was added and incubated for 5 min. Then the mixture was applied to a QIAamp MinElute column and centrifuged at 6,000× g for 1 min at room temperature. Flow-through was discarded and the column was subsequently washed and DNA was eluted by adding 20 µl of Buffer AE and centrifugation at 20,000× g for 1 min.

Polymerase chain reaction (PCR) and DNA sequencing

Touchdown PCR was performed using a PCR Thermal Cycler DICE (TaKaRa, Kyoto, Japan) as described previously [26]. PCR primers were designed to be specific to the *M. leprae* genome and were used in previous studies [24,27,28]; all the primers are listed in Table 2. The PCR products were analyzed by 2% agarose gel electrophoresis. Nested PCR was used to amplify *hsp-70*, *16S rRNA* and SNPs. Some of the results were confirmed in an independent laboratory.

The DNA sequence was analyzed using an ABI PRISM 310 Genetic Analyzer and GeneScan Collection software (Applied Biosystems).

Whole genome amplification (WGA)

A GenomePlex Whole Genome Amplification kit (Sigma, St Louis, MO) was used to amplify genomic DNA samples according to the manufacturer's protocol [29]. Briefly, 1 µl of 10× Fragmentation Buffer was mixed with 10 µl of DNA solution and incubated for 4 min at 95°C. After cool down, 2 µl of 1× Library Preparation Buffer and 1 µl of Library Stabilization Solution were added and incubated for 2 min at 95°C. Then 1 µl of 1× Library Preparation Enzyme was added and incubated at 16°C for 20 min, at 24°C for 20 min, at 37°C for 20 min and at 75°C for 5 min to ensure library preparation. To amplify genomic DNA, 7.5 µl of 10× Amplification Master Mix, 47.5 µl of Nuclease-free Water and 5 µl of Jumpstart *Taq* DNA polymerase were added and heated at 95°C for 3 min, then 14 cycles of two-temperature amplification was employed at 94°C for 15 sec and 65°C for 5 min using a PCR Thermal Cycler DICE (TaKaRa). The quality of the WGA products was evaluated by 1% agarose gel electrophoresis.

Others

All experiments were performed in a biosafety level 2 (BSL2) laboratory where samples were handled in a safety cabinet using disposable sterile materials to avoid any contamination.

Results

Demonstration of *M. leprae* DNA by PCR and DNA sequencing

The purified DNA from seven different sites of skeletons from three individuals was subjected to PCR amplification of the *M. leprae*-specific *hsp-70* gene and *16S rRNA* genes. A nested PCR protocol to amplify the *M. leprae*-specific *16S rRNA* region was developed in our laboratory. Among four samples taken from

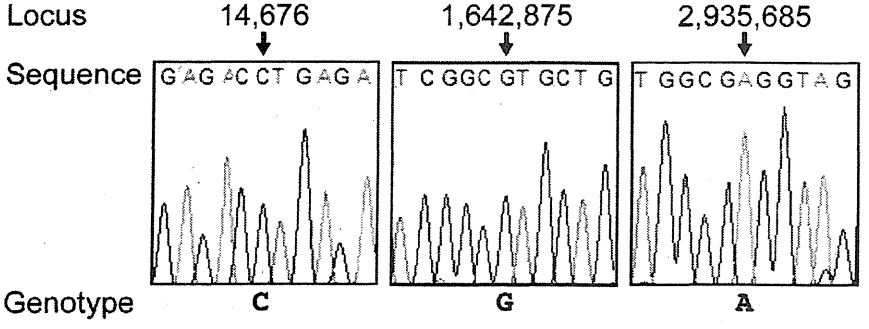

Figure 4. Sequence analysis of the three reported SNPs of *M. leprae* DNA. Each locus was PCR amplified and sequenced as described in the Materials and Methods.
doi:10.1371/journal.pone.0012422.g004

leprous lesions, a specific positive signal was derived from sample No. 1 (right maxillary palate of SK26) and No. 4 (right fibula of SK26), but not from the others (Fig. 3). Samples taken from control bones were all negative. Human *β-globin* DNA was detected by PCR only from sample No. 7 (lower premolar root of SK16).

The specificity of these PCR amplifications was confirmed by DNA sequencing of the PCR products purified from agarose gel. Basic Local Alignment Search Tool (BLAST) search of the DNA sequence was a 100% match with the reported *M. leprae* sequence for both *hsp-70* and *16S rRNA* as expected (data not shown). The results clearly confirmed that *M. leprae* was involved in the skeletal lesions of SK26 diagnosed as lepromatous leprosy.

SNP analysis of the *M. leprae* DNA

To determine the possible origin of the *M. leprae* found in this skeleton, we analyzed single-nucleotide polymorphisms (SNPs) at 3 reported loci in the *M. leprae* genome [2,3]. PCR amplification followed by direct sequencing identified the sequence at the 3 loci. Positions 14,676, 1,642,875 and 2,935,685, were "C", "G" and "A", respectively (Fig. 4). This genotype of *M. leprae* DNA is reported as SNP type 1, which is the dominant type in India and Southeast Asia [2,3].

Evaluation of WGA-PCR method

We have attempted to amplify other regions of the *M. leprae* genome using PCR primers we have designed previously [27] and found that the sensitivity to detect *M. leprae* DNA from ancient samples is significantly lower than from the clinical samples we analyze in our laboratory. To solve this problem, we have applied WGA to amplify whole genomic DNA purified from skeletal samples. Purified DNA from sample No. 1 was subjected to WGA and the DNA before and after WGA was compared by PCR using 19 different PCR primers targeting open reading frames, pseudogenes and non-coding regions of the *M. leprae* genome [24,27]. WGA-amplified DNA was positive for 15 sets of PCR primers, while *M. leprae* genomic DNA was detected by only 7 primer sets in the original DNA sample (Fig. 5), showing that WGA-PCR has superior sensitivity over conventional PCR.

Discussion

We have demonstrated *M. leprae* DNA in excavated human skeletal remnants from Japan by both PCR analysis and DNA sequencing. We also sequenced three SNPs in the *M. leprae* DNA and confirmed that the bacilli are of the dominant type in Southeast Asia. Although *M. leprae* DNA has already been found in archaeological bone remains in Europe and the Middle East [13,14,15,16,17,18,19,20,21], there have been no reports from Far East Asia. This may be related to the geographical and environmental diversity between Europe and Asia, where archaeologists and anthropologists have not paid much attention to palaeopathological topics of leprosy and other infectious diseases [22]; Asia's predominantly hot and humid climate may cause difficulty in recovering skeletons buried for several hundred years.

The present case was excavated in the northern part of Japan and showed typical osteological changes of leprosy. We took skeletal samples from four different areas, the inner surface of the nasal cavity, maxillary palate and diaphysis of the fibula, that showed deformities by erosion and atrophy, or mild periostitis. *M. leprae* DNA was successfully demonstrated in the maxillary palate and fibular diaphysis.

Although subperiostal exostoses and/or hypertrophy accompanied by swelling or porotic hyperosteosis of the fibula are reported as the typical signs of leprosy [6,7], the presence of *M. leprae* DNA in the fibula was somewhat surprising to us because apparent fibular lesion is not common in leprosy patients at present. It is well known that the common fibular nerve is one of the sites preferably affected by *M. leprae*, which causes foot drop in the patient [30]. It may therefore be possible to speculate that *M. leprae* affected the periosteum through this nerve. If that is the case, the present identification of *M. leprae* DNA in the fibula supports the possibility that *M. leprae* can spread significantly throughout the body when patients are left untreated.

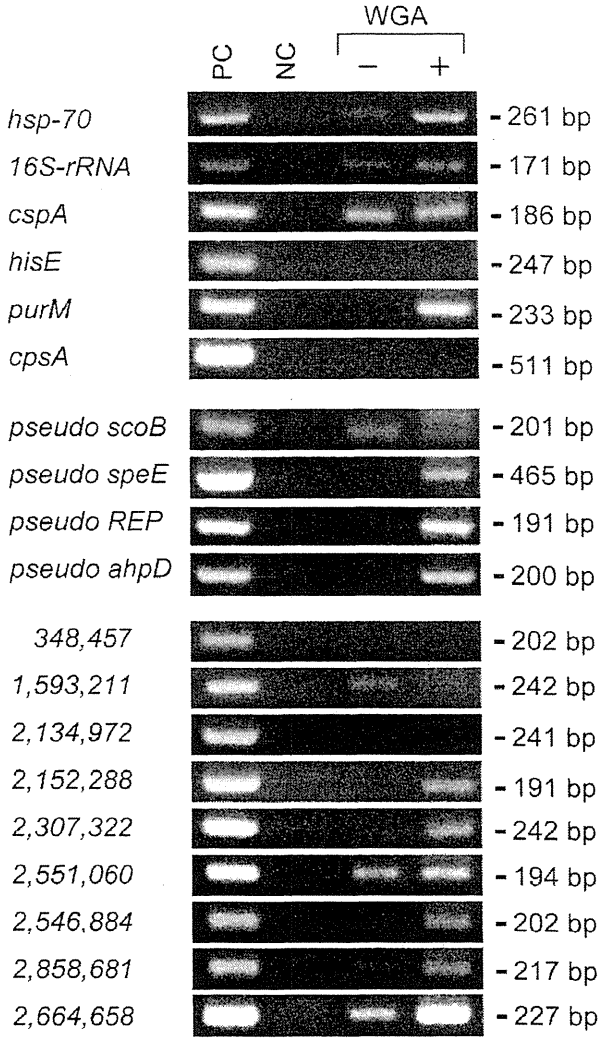

Figure 5. Comparison of conventional PCR and WGA-PCR. PCR was performed using a DNA sample derived from the present study (sample No. 1 shown in Table 1 and Fig. 3). The DNA before and after WGA ("−" and "+", respectively) was amplified using specific nested primers and direct primers targeted for the genes, pseudogenes and non-coding regions of *M. leprae* genome as listed in Table 2. Names of the genes and pseudogenes are indicated and the coordinate positions of non-coding regions in the genome (http://genolist.pasteur.fr/Leproma/) are indicated numerically. PC: positive control DNA from *Thai 53* strain of *M. leprae*; and NC: negative control using DNase/RNase-free water instead of a DNA sample for PCR reaction.
doi:10.1371/journal.pone.0012422.g005

The SNP genotype of *M. leprae* DNA in *Hatanai* SK26 was type 1, which is a major group in Southeast Asia and India, but rather minor in modern East Asia including Japan and China [2,3]. All reported SNP types of ancient *M. leprae* DNA from Europe and Middle East are type 3, which is also a major genotype in the same regions at present [3]. However, this study confirmed the first case of SNP type 1 as ancient DNA samples. Although more evidence is required, this suggests the possibility that in the Far East inclusive of Japan, the dispersal process of the phylogenetic type of leprosy is historically different from the occidental world. In the Southeast Asia and India where the modern dominant SNP group is type 1, archaeological skeletal remains with lesions of lepromatous leprosy have been excavated and dated from ca. 2000 BC (India) to ca. 300 BC-500 AD (Thailand) [31,32]; therefore the type 1 genotype in modern Japan might be traced back to Southeast Asia and probably originated in India. A historical record of ancient Japan mentioned that the oldest case suggestive of leprosy dated back to the 7th century, and the oldest positive palaeopathological evidence at present is dated to the 13th century. The genotypes of these ancient and medieval materials are still unknown, and further examination of ancient materials from Eastern and Southeast Asia are needed in order to determine the dispersal history of leprosy in Far East Asia.

In our laboratory, PCR detection of *M. leprae* DNA is routinely performed from small amounts of clinical samples of skin smears or paraffin sections as part of a government reference center. It is difficult, however, to apply the same PCR protocol to detect *M. leprae* from ancient DNA recovered from skeletal remains. To overcome this problem, we have utilized WGA, a technique that enables amplification of minute amounts of DNA [29], to increase the sensitivity for PCR detection. We have successfully utilized this method to amplify and detect environmental bacteria from small amounts of water taken from the sea or lakes in Japan (unpublished data).

By PCR reaction using WGA-amplified DNA (WGA-PCR method), large amounts of DNA could be generated from minute amounts of original DNA samples and the detection rate of *M. leprae* DNA and signal intensity were significantly improved. Thus, this method enables highly sensitive detection of small amounts of clinical, environmental and ancient DNA. On the other hand, it also carries the risk of contamination and false positives, particularly if performed by an individual lacking appropriate knowledge and training in molecular biology. Even using this method, however, some primers still did not work on ancient DNA. This might be due to DNA fragmentation in the ancient sample and/or because of the DNA fragmentation process employed during the library preparation step in the WGA protocol. In general, genomic DNA from dead organisms gradually degrades into short fragments over time mainly due to the activity of nucleases produced by microorganisms in the soil. PCR detection, even using the present WGA-PCR method, will be difficult to perform when such a fragmentation proceeds, especially for very old materials and those buried in conditions where the decomposition process is accelerated, *e.g.* a hot and humid environment. Nevertheless, WGA-PCR seems to be advantageous for improving the sensitivity of DNA recovery from these samples. We are now routinely utilizing this method to detect ancient DNA and believe that it will be applicable for detecting other kinds of DNA from archaeological samples, as well as other kinds of samples with trace amounts of DNA.

Acknowledgments

The authors wish to thank Drs. Toshio Yanagida and Jun Nemoto (Tohoku University Museum) for permission to obtain the sample materials. We also appreciate the contribution of Drs. Junya Sakurai (Shobi University), Aiko Saso (The University of Tokyo), and Keigo Hoshino and Kazuaki Hirata (St. Marianna University) for to discussion.

Author Contributions

Conceived and designed the experiments: KS NI. Performed the experiments: KS WT KT KN YI AK HW SM. Analyzed the data: KS TA MS AY. Contributed reagents/materials/analysis tools: KS TA MS AY. Wrote the paper: KS WT NI.

References

1. Cole ST, Eiglmeier K, Parkhill J, James KD, Thomson NR, et al. (2001) Massive gene decay in the leprosy bacillus. Nature 409: 1007–1011.
2. Monot M, Honore N, Garnier T, Araoz R, Coppee JY, et al. (2005) On the origin of leprosy. Science 308: 1040–1042.
3. Monot M, Honore N, Garnier T, Zidane N, Sherafi D, et al. (2009) Comparative genomic and phylogeographic analysis of *Mycobacterium leprae*. Nat Genet 41: 1282–1289.
4. Carpintero P, Logrono C, Carreto A, Carrascal A, Lluch C (1998) Progression of bone lesions in cured leprosy patients. Acta Leprol 11: 21–24.
5. Coutelier L (1971) The bone lesions in leprosy. A study based on microradiography and fluorescence microscopy. Int J Lepr Other Mycobact Dis 39: 231–243.
6. Boldsen JL (2008) Leprosy in the early medieval Lauchheim community. Am J Phys Anthropol 135: 301–310.
7. Boldsen JL, Mollerup L (2006) Outside St. Jorgen: leprosy in the medieval Danish city of Odense. Am J Phys Anthropol 130: 344–351.
8. Aufderheide AC, Rodriguez-Martin C (1998) The Cambridge Encyclopedia of Human Paleopathology. Cambridge: Cambridge University Press.
9. Ortner DJ (2003) Identification of Pathological Conditions in Human Skeletal Remains. London: Academic Press.
10. Roberts C, Manchester K (2007) The Archaeology of Disease. New York: Cornell University Press.
11. Drancourt M, Raoult D (2005) Palaeomicrobiology: current issues and perspectives. Nat Rev Microbiol 3: 23–35.
12. Spigelman M, Lemma E (1993) The use of the polymerase chain reaction to detect Mycobacterium tuberculosis in ancient skeletons. Int J Osteoarchaeol 3: 143.
13. Rafi A, Spigelman M, Stanford J, Lemma E, Donoghue H, et al. (1994) *Mycobacterium leprae* DNA from ancient bone detected by PCR. Lancet 343: 1360–1361.
14. Watson CL, Lockwood DN (2009) Single nucleotide polymorphism analysis of European archaeological *M. leprae* DNA. PLoS One 4: e7547.
15. Donoghue HD, Marcsik A, Matheson C, Vernon K, Nuorala E, et al. (2005) Co-infection of Mycobacterium tuberculosis and *Mycobacterium leprae* in human archaeological samples: a possible explanation for the historical decline of leprosy. Proc Biol Sci 272: 389–394.
16. Montiel R, Garcia C, Canadas MP, Isidro A, Guijo JM, et al. (2003) DNA sequences of *Mycobacterium leprae* recovered from ancient bones. FEMS Microbiol Lett 226: 413–414.
17. Haas CJ, Zink A, Palfi G, Szeimies U, Nerlich AG (2000) Detection of leprosy in ancient human skeletal remains by molecular identification of *Mycobacterium leprae*. Am J Clin Pathol 114: 428–436.
18. Taylor GM, Widdison S, Brown IN, Young D (2000) A mediaeval case of lepromatous leprosy from 13-14 century Orkney, Scotland. J Archaeol Sci 27: 1133–1138.
19. Donoghue HD, Gladykowska-Rzeczycka J, Marscik A, Holton J, Spigelman M (2002) Mycobacterium leprae in archaeological samples. In: Roberts CA, Lewis ME, Manchester K, eds. The Past and Present of Leprosy: Archaeological, Historical, Palaeopathological and Clinical Approaches. Oxford: British Archaeological Reports. pp 271–285.
20. Taylor GM, Watson CL, Lockwood DNJ, Mays SA (2006) Variable nucleotide tandem repeat (VNTR) typing of two cases of lepromatous leprosy from the archaeological record. J Archaeol Sci 33: 1569–1579.
21. Likovský J, Urbanová M, Hájek M, Černý V, Čech P (2006) Two cases of leprosy from Žatec (Bohemia), dated to the turn of the 12th century and confirmed by DNA analysis for *Mycobacterium leprae*. J Archaeol Sci 33: 1276–1283.
22. Blau S, Yagodin V (2003) Osteoarchaeological evidence for leprosy from western Central Asia. Am J Phys Anthropol 126: 150–158.
23. Takigawa W, Kawakubo Y, Maeda T, Sakaue K, Saeki F, et al. (2002) Early modern skeletal remains excavated from Hatanai site in Nango Village, Aomori Prefecture. In: Educational Board of Aomori Prefecture ed. Hatanai site VIII Archaeological Investigation Report of Aomori Prefecture 326. Aomori: Aomori Prefecture. pp 254–282. (in Japanese).

24. Akama T, Suzuki K, Tanigawa K, Kawashima A, Wu H, et al. (2009) Whole-genome tiling array analysis of *Mycobacterium leprae* RNA reveals high expression of pseudogenes and noncoding regions. J Bacteriol 191: 3321–3327.
25. Suzuki K, Nakata N, Bang PD, Ishii N, Makino M (2006) High-level expression of pseudogenes in *Mycobacterium leprae*. FEMS Microbiol Lett 259: 208–214.
26. Tanigawa K, Suzuki K, Nakamura K, Akama T, Kawashima A, et al. (2008) Expression of adipose differentiation-related protein (ADRP) and perilipin in macrophages infected with *Mycobacterium leprae*. FEMS Microbiol Lett 289: 72–79.
27. Nakamura K, Akama T, Bang PD, Sekimura S, Tanigawa K, et al. (2009) Detection of RNA expression from pseudogenes and non-coding genomic regions of *Mycobacterium leprae*. Microb Pathog 47: 183–187.
28. Suzuki K, Udono T, Fujisawa M, Tanigawa K, Idani G, et al. (2010) Infection during infancy and long incubation period of leprosy suggested in the case of a chimpanzee used for medical research. J Clin Microbiol, July 14 [Epub ahead of print].
29. Barker DL, Hansen MS, Faruqi AF, Giannola D, Irsula OR, et al. (2004) Two methods of whole-genome amplification enable accurate genotyping across a 2320-SNP linkage panel. Genome Res 14: 901–907.
30. Soysal A, Atay T, Ozu T, Arpaci B (2004) Electrophysiological evaluation of peripheral and autonomic involvement in leprosy. Can J Neurol Sci 31: 357–362.
31. Robbins G, Tripathy VM, Misra VN, Mohanty RK, Shinde VS, et al. (2009) Ancient skeletal evidence for leprosy in India (2000 B.C.). PLoS One 4: e5669.
32. Tayles N, Buckley HR (2004) Leprosy and tuberculosis in Iron Age Southeast Asia? Am J Phys Anthropol 125: 239–256.

JOURNAL OF CLINICAL MICROBIOLOGY, Sept. 2010, p. 3432–3434 Vol. 48, No. 9
0095-1137/10/$12.00 doi:10.1128/JCM.00017-10

Infection during Infancy and Long Incubation Period of Leprosy Suggested in a Case of a Chimpanzee Used for Medical Research▽

Koichi Suzuki,[1]* Toshifumi Udono,[2] Michiko Fujisawa,[3] Kazunari Tanigawa,[1] Gen'ichi Idani,[3] and Norihisa Ishii[1]

Leprosy Research Center, National Institute of Infectious Diseases, Tokyo, Japan[1]; Chimpanzee Sanctuary Uto, Sanwa Kagaku Kenkyusho, Kumamoto, Japan[2]; and Department of Welfare and Longevity Research, Wildlife Research Center, Kyoto University, Kyoto, Japan[3]

Received 5 January 2010/Returned for modification 25 February 2010/Accepted 6 July 2010

The length of the incubation period of leprosy following *Mycobacterium leprae* infection has never been conclusively determined, owing to the lack of a method to demonstrate the presence of an asymptomatic infection. We report a rare case of leprosy in a chimpanzee in which a 30-year incubation period was strongly suggested by single nucleotide polymorphism (SNP) analysis.

CASE REPORT

A female chimpanzee (*Pan troglodytes*) named Haruna was caught in Sierra Leone, West Africa, and brought to Japan in 1980 when she was around 2 years old. She was used in hepatitis B studies for 6 years and in hepatitis C studies for another 4 years before she was retired to live out her life in a sanctuary. She and her fellow chimpanzees were kept according to the guidelines of Chimpanzee Sanctuary Uto, Wildlife Research Center, Kyoto University, Japan. Resident chimpanzees are treated with the same level of care as human patients in hospitals, and all physical examinations were carried out solely for the purpose of diagnosis and treatment, as approved by the sanctuary. Despite her experimental history, she is seronegative for HBsAg, HBs antibody (HBsAb), and HBcAb, as well as for the presence of hepatitis C virus (HCV) RNA. Results of other laboratory tests were all normal.

In January 2009, at around age 31 (the average life span of a chimpanzee is 40 to 50 years and rarely exceeds 50 years), swellings and nodules (Fig. 1A) that had not been observed in the past were noted on her face (Fig. 1B). A thorough examination under anesthesia revealed multiple nodular lesions around the eyes, lips, abdomen, forearms, and crus. Nasal swabs and skin smears from a forearm nodule revealed a large number of acid-fast bacilli, with formation of globi (Fig. 1C and 1D, respectively). Results of a skin tuberculosis (TB) test were negative. Histologic examination of the skin lesion showed a granulomatous accumulation of foamy histiocytes in the upper dermis that contained numerous acid-fast bacilli (Fig. 1E and F) that were positive for PGL-I immunostaining (PGL-I is an antigen specific to *Mycobacterium leprae*). PCR amplification of DNA purified from a skin biopsy sample was positive for *M. leprae*-specific Hsp70 (Fig. 1G), and the DNA sequence of 16S rRNA completely matched the reported *M. leprae* sequence (2).

At this point, a diagnosis of lepromatous leprosy was made and the patient was treated with multidrug therapy (MDT), including diaphenylsulfone, clofazimine, and rifampin, according to the protocol of the World Health Organization (WHO). These drugs were administered after being mixed with bananas or vegetable juice. Within 2 months of treatment, the skin lesions had significantly improved, and within 5 months, nasal swabs tested negative for acid-fast bacilli.

To determine the possible origin of *M. leprae* detected in this case, we analyzed single nucleotide polymorphisms (SNPs) for three reported loci in the *M. leprae* genome (13). By using PCR amplification followed by direct sequencing, positions 14,676, 1,642,875, and 2,935,685 of *M. leprae* DNA were identified as "T," "T," and "C," respectively (Fig. 2). This genotype, which has been identified only in West Africa, was classified as SNP type 4; it is thought to have been introduced to parts of the Caribbean and South America, probably via the slave trade, but has not been identified in Japan or other Asian countries (13, 14).

Increased levels of serum anti-PGL-I antibody have been used for the diagnosis of lepromatous leprosy (1). High levels of serum anti-PGL-I antibody have also been reported in healthy household contacts in an area where the disease is endemic (7). However, there have been some arguments about the specificity of PGL-I for leprosy as well as about the clinical relevance of measuring the level of anti-PGL-I antibody for the diagnosis of leprosy, particularly for the detection of subclinical *M. leprae* infection (9). The results of analysis of archived serum samples from Haruna were negative for anti-PGL-I antibody until 25 October 2007 (ca. 1 year before her skin lesions were observed) and became positive on 13 May 2009, after the appearance of skin lesions, but returned to negative on 8 October 2009, approximately 5 months after MDT was administered (Fig. 3). Eight other chimpanzees imported to Japan in the same year and five others living in the same cage with Haruna for several years were all negative for serum anti-PGL-I antibody.

Leprosy has afflicted humans for millennia and is caused by chronic infection with *M. leprae*. It is believed that the disease

* Corresponding author. Mailing address: Leprosy Research Center, National Institute of Infectious Diseases, 4-2-1 Aoba-cho, Higashimurayama-shi, Tokyo 189-0002, Japan. Phone: 81-42-391-8211. Fax: 81-42-394-9092. E-mail: koichis@nih.go.jp.

▽ Published ahead of print on 14 July 2010.